Melting heat transfer in the flow of Carreau nanofluid past a stretching cylinder in a Darcy-Forchheimer porous medium

Thesis Submitted By

Hafeez Akhter
(01-248182-007)

Supervised By

Prof. Dr. M. Ramzan

A dissertation submitted to the Department of Computer Science, Bahria University, Islamabad as a partial fulfillment of the requirements for the award of the degree of MS

Session (2018 - 2020)

Bahria University
Discovering Knowledge

MS-13

Thesis Completion Certificate

Student's Name: **Hafeez Akhter** Registration No. **59378**
Program of Study: **MS(Mathematics)**
Thesis Title: **"Melting heat transfer in the flow of Carreau nanofluid past a stretching cylinder in a Darcy Farchheimer porous medium"**

It is to certify that the above student's thesis has been completed to my satisfaction and, to my belief, its standard is appropriate for submission for Evaluation. I have also conducted plagiarism test of this thesis using HEC prescribed software and found similarity index at **17%** that is within the permissible limit set by the HEC for the MS/MPhil degree thesis. I have also found the thesis in a format recognized by the BU for the MS/MPhil thesis.

Principal Supervisor's Signature: ______________________

Date: 17-09-2020 **Name: Prof. Dr. M. Ramzan**

Dedicated to

My beloved parents and respected supervisor

Acknowledgments

Words are bound and knowledge is limited to praise **ALLAH** the beneficent, the merciful who universe and bestowed mankind with the knowledge and ability to think into his secrets. Then the trembling lips and wet eyes praise the greatest man of universe, the last messenger of **ALLAH, HAZRAT MUHAMMAD (PBUH)**, whom **ALLAH** has sent as mercy for worlds, the illuminating torch, the blessing for the literate, illiterate, rich, poor, powerful, weaker, and able and disable.

My acknowledgment is to my kind, diligent and highly zealous supervisor, Prof. Dr. M. Ramzan, who supported me with his cherished opinions and inspirational discussions. His valuable expertise, comments, suggestions and instructions are most welcome that greatly improved the clarity of this document.

My gratitude is to my honorable professors who took me to the apex of my academia with their guidance. In particular, Dr. Rizwan-ul-haq and Dr. Jafar Hasnain who have always been supportive in all of my course work and kept encouraging me throughout the session in Bahria University, Islamabad Campus. They are the true teachers who have made Mathematics Department of BUIC, a real place of learning.

My intense recognition is to my Parents, brothers and sister, who are always real pillars for my encouragement and showered their everlasting love, care and support throughout my life. I am very grateful to Ma'am Hina Gul and Ma'am Saima who support and guided me at every stage, my seniors Sania Naseer and Nazia Shahmir, and my friend Muhammad Usman khan were specially remained enormously helpful throughout the period of my MS studies.

Hafeez Akhter

Bahria University Islamabad, Pakistan

September 2020

Bahria University
Discovering Knowledge

MS-14A

Author's Declaration

I, **Hafeez Akhter** hereby state that my MS thesis titled **"Melting heat transfer in the flow of Carreau nanofluid past a stretching cylinder in a Darcy Farchheimer porous medium"** is my own work and has not been submitted previously by me for taking any degree from this university **Bahria University Islamabad** or anywhere else in the country/world.

At any time if my statement is found to be incorrect even after my Graduate the university has the right to withdraw/cancel my MS degree.

Name of scholar: **Hafeez Akhter**

Date: **17/09/2020**

Bahria University
Discovering Knowledge

MS-14B

Plagiarism Undertaking

I solemnly declare that research work presented in the thesis titled "**Melting heat transfer in the flow of Carreau nanofluid past a stretching cylinder in a Darcy Farchheimer porous medium**" is solely my research work with no significant contribution from any other person. Small contribution / help wherever taken has been duly acknowledged and that complete thesis has been written by me.

I understand the zero tolerance policy of the HEC and Bahria University towards plagiarism. Therefore I as an Author of the above titled thesis declare that no portion of my thesis has been plagiarized and any material used as reference is properly referred / cited.

I undertake that if I am found guilty of any formal plagiarism in the above titled thesis even after award of MS degree, the university reserves the right to withdraw / revoke my MS degree and that HEC and the University has the right to publish my name on the HEC / University website on which names of students are placed who submitted plagiarized thesis.

Student / Author's Sign:______________

Name of the Student: **Hafeez Akhter**

Abstract

This mathematical analysis refined, the transfer of melting heat in the flow of Carreau nanoliquid via a stretched cylinder is examined. Moreover, the phenomenon of flow is conducted in the existence of Darcy-Farchheimer porous medium. The nanofluid flow is also discussed in the existence of gyrotactic microorganisms. The governing equations of boundary layer are transformed into non-linear ODEs after applying appropriate similarity transformation. The resulting system of linear equations is addressed by bvp4c built-in function of MATLAB scheme. The outcomes of the prominent parameters versus emerging profiles are portrayed and conversed in the light of their physical significance.

LIST OF TABLES

LIST OF FIGURES

NOMENCLATURE

x, r	Coordinate axis
u, v	Velocity components
μ	Dynamic viscosity
F_i	Components of force
A_j	Components of area
τ_{ji}	Stress
ρ	Density of fluid
η_1	Apparent viscosity
v	Velocity component along 'r' directions
k_1	Consistency index /Inertial permeability
m	Mass of substance
V	Volume
P	Pressure
α	Thermal diffusivity
K	Thermal conductivity
C_p	Specific heat capacity
C_s	Heat capacity of solid surface
Q_1	Heat transferred of a ratio

ΔT	Temperature difference
τ	Cauchy stress tensor
I	Identity tensor
A_1	First Rivlin-Ericksen tensor
μ_0	Zero shear rate viscosity
μ_∞	Infinite shear rate viscosity
n	Power law index
Γ	Material time constant
$\gamma^{\cdot}$	Share rate
Π	Second invariant strain tensor
v_f	Forchheimer velocity
Pr	Prandtl number
v	Momentum diffusivity
D_B	Brownian diffusion coefficient
Le	Lewis number
T_w	Constant temperature
T_∞	Temperature outside the plate / Free stream temperature
Nb	Brownian motion parameter
Nt	Thermophoresis parameter
D_T	Thermophoresis coefficient
We	Weissenberg number

Fr	Darcy parameter
C_∞	Concentration in the free stream
β^*	Non–Darcian coefficient
K^*	Permeability of porous medium
U_0	Reference velocity
l	Characteristics length
Pe	Peclet number
Wc	Constant maximum cell swimming speed
Dn	Diffusivity of the microorganism
λ	Porosity Parameter
T_m	Melting temperature
T_0	Solid temperature
τ_{rx}	Shear stress
U_w	Axial route having velocity
C_{fx}	Skin friction
N_{ux}	Nusselt number
Sh_x	Sherwood number
N_{nx}	Density number of motile microorganisms
q_w	Surface heat flux
b	Body force

q	Heat flow
$\frac{dT}{dx}$	Temperature gradient
$\frac{du}{dy}$	Velocity gradient
$\frac{d}{dt}$	Material time derivative
σ^*	Stephen – Boltzmann's constant
h	Coefficient heat transfer
T_s	System temperature
e	Emissivity of the system
γ^2	Curvature parameter
M	Melting parameter

Contents

Chapter 1

Introduction and literature review

1.1 Introduction

Modern enhancements in industrial applications necessitated a broad variety of non-Newtonian liquids which are derived from the viscous liquids. All those liquids in which the rate of shear is changed and the shear stress remain unchanged, are considered to be non-Newtonian liquids. Hence, the change in the shear strength alter the viscosity of these liquids, which is also known the "apparent viscosity" of the liquid. The study of non-Newtonian liquids have significant part in various engineering and industrial processes, for example, paper production, petroleum drilling, glass blowing, plastic sheet formation, the expulsion of polymeric liquids and melts, biological solutions, asphalts, paints and so forth. These liquids are expressed as materials that do not show the direct or linear correspondence between shear stress and velocity gradient. For this class of liquids, an infinite possible rheological relationships exist. Rheological characteristics of non-Newtonian liquids differ a lot in comparison to the Newtonian liquids. No doubt, the rheological characteristics of all the non-Newtonian liquids can't be expressed by a single constitutive equation exhibiting rates of shear and rate of strain. As for non-Newtonian liquids, there is always a non-linear relationship among the stress and the rate of strain. The governing constitutive equations in non-Newtonian liquids are much complicated, nonlinear and of more higher order in constrast to the Newtonian liquids. These liquids can conveniently be categorized into three main classes i) Liquids for that the shear rate at any spot is calculated only via the variation of the shear stress at that spot, these liquids are commonly known the "time independent", "inelastic", "purely viscous" or "generlized Newtonian liquids". ii) Much complicated liquids for that the relationship among the shear stress and the rate of shear depends on the timmings of shearing and their kinematic history, known as "time dependent liquids". iii) Materials exhibiting the properties of one as well as the other ideal liquids and elastic solids and displaying partial elastic recovery and later the deformation they are categorizesd as "Visco-elastic liquids".

The classifying scheme of these liquids is arbitrary among most real materials which exhibit a mixture of two or even all three types of non-Newtonian properties. This assumption is too extensive to be tackled in the starting phases of the development. So, a particular rheological model will be selected for use to start with, and application of the outcoming development to liquids departing from the assumed model will be considered eventually. A considerable work has been completed in the system of non-Newtonian liquids and a lot of more is required in an assortment of non-Newtonian liquid models. Various self-consistent and approximate non-Newtonian rheological models are proposed over the past decades as no individual one can encompass assorted properties of all the liquids. These models are restricted into differential, rate and integral types. Because of related simplicity of the Power law model it has been concentrated by various scientists all together to explore non-Newtonian impacts. In any case, the law of Power model has it restrictions. In consideration of the impediments of the Power law model, particularly for extremely up and down rates of shear, here we assume another viscosity model which is known as Carreau liquid model. Carreau liquid is a kind of generalized Newtonian liquid where viscosity relies on the rate of shear. The Carreau model is valuable in illustrating the behavior of flow of liquids in the higher rate of shear.

The nanoliquid is a liquid that contains nanometer sized material particles, called nanoparticles. The nano particles used in nanoliquids are usualy made up of metals, oxides, or carbon nanotubes. The nanofluids are different from other ordinary base fluids because they are prepared by inserting nanoparticles in the base fluids. Simple base liquids are like water, ethylene glycol and oil. These particles are inserted into base liquids to increase the thermal conductivity and phenomenon of heat transfer. Nanoliquid is an ideal applicant to get position of working liquid and having thermal conductivity greater than the base liquid and a size of 1 to 100 nm. These substances are used to get the significant improvement in the thermal properties at lower concentrations. Nanoliquids have the potential to enhance the rates of heat transfer significantly in a various of zones like nuclear reactors, industrial cooling applications, transportation industry, heat exchangers, micro-electromechanical systems, fiber and granular insulation, chemical catalytic reactors, packed flow of blood in the cardiovascular system engaging the Navier–Stokes equations. The advanced characteristics of naofluid has important value in many fields as transportation, pharmaceutical processes, microelectronics, power generation, micro manufacturing, thermal therapy for air-conditioning, cancer surgery, chemical sectors and metallurgical processes etc. In vehicles, the worth of nanofluids as coolants takes into consideration for good size and consequently this consumes smaller energy for controlling the road resistance. Many current researchers are working to grow efficient solar collectors with up absorpation of solar radiations.

Compared to base liquids, nano liquids are heat transfer liquids of next generation because they provide exciting new posiibilities to improve heat transfer efficiency. In 1856, Henri Darcy (a French civil engineer) in his publication presented the quantitative theory of the flow of homogenous fluids through spongy media.and studied the characteristics of sand filters for water filtering in the city of France. After these studies and experiments, he came forward with the result that "viscous forces dominate over inertial forces in porous media" which came to be known as Darcy Law, globally. Darcy Law model are the following characteristics:

- Darcy law considers laminar or viscous flow (creep velocity); inertia term (the fluid density) do not involve in it. This depicts that the inertia forces in the liquid are being ignored which was not the case in classical Navier-Stokes equation theory.

- Darcy law has this inherent supposition that in a poriferous media a vast surface area is subject to liquid flow, as a result the viscosity will significantly surpass acceleration forces in the liquid unless turbulence is experienced.

With vast utilization in grain stockpiling, petroleum technology, frameworks of ground water and oil assests, this law of immense importance in the field of Fluid Mechanics. Places where the porous media have greater rates of flow due to non-uniformity, such as close to the wall, Darcy law is not applicable. Keeping this in mind, one has to become mindful of the non-Darcian influence by porous media in the flow analysis and rate of heat transfer. A Dutch man named

Philippe Forcchheimer, in 1901, while flowing gas thorough coal beds revealed that the relation between rate of flow and potential gradient is non-linear at comparatively greater velocity, and that non-linearity witnesses surge with increase in flow rate. Forcchheimer at the time was of view that this non-linear increase was as a outcome of turbulence in the fluid flow but it is now renowned that this non-linearity is due to inertial effects in the spongy media. However for increased flow rate, the methodology of Forchheimer expression is deliberated. Forchheimer resulted in an advanced relation known Darcy Forchheimer expression, by letting a quadratic term in equation of motion. This term that was always there for a large Reynolds number was called as Forcheimer term by Muskat in 1946. Physically, quadratic drag for spongy media in momentum equation occurs for more filtration velocities, cause to solid obstructs this drag is formed and becomes identical with drag at the surface by resistance. There are numerous examples of the possible situations of practical applications where the inertial effects can be important and Darcy's law is no longer exist. For these situations, one may refer liquid flows in column reactors, in aquifers and in filters etc.

1.2 Literature review

With the efficient progress of recent science and technology, the nano-materials as a type of new materials has got exclusive attention by various research workers. A liquid holding nanometer-sized particles is known as nanofluid. The nanofluids consist of nano particles generally along with carbon nanotubes, metals or oxides. Nanoliquids are dstinct from other ordinary base liquids because they are analyzed by diffusing nanoparticles in the base liquids. Oil, water ethylene and glycol are the simply used base liquids. The material particles are inserted into the base fluids to boost their heat transfer performance and thermal conductivity. Such liquids are mostly used in transport of electronics, fiber technology, transportation, textile and energy production. Furthermore, the magneto-nanoliquid has significant importance in making of loud speakers, blood analysis and cancer treatment. Nanoliquid is an ideal applicant to get the title of the working liquid. Many researchers are working on nano-liquids with different heat transit properties. Recently, Sheikholeslami et al. [1] examined the effect of rotating materials into the hydraulic thermal performance of a flow of nanoliquid via a tube. Ramzan et al. [2] discussed the magneto radiative Micropolar nanoliquid flow with binary chemical species, activation energy and double stratification under the buoyancy effects. Yang et al. [3] worked on the analysis of a newly combined application of nanoliquids in heat recovery and air purification. Various studies have been conducted to expose the various aspects of the nanliquid in [4-15].

Viscoelastic fluids have accomplished exclusive enthusiasm by current researchers in perspective of more extensive mechanical and engineering applications. The investigations on these liquids are extensively increased during the last some decades because of their practical significance in technology and industrial processes. Most of the substances in our regular life include apple sauce, sugar solution, muds, chyme, soaps, emulsion, shampoos, blood at low shear rates. The analysis of non-Newtonian materials has engrossed continuous consideration of recent investigators. The influence of non-Newtonian fuids in the industry is more imperious in comparison to Newtonian liquids owing to their utility in varied applications [16]. Examples of non-Newtonian liquids may embrace coal water, paints, asphalt, toothpaste, and jellies etc. [17]. In literature, there is no individual relationship that characterizes all the properties of non-Newtonian liquids. Thus various models of non-Newtonian liquids have been suggested. The Carreau nanoliquid is the mixture of the Newtonian and Power-law models. This liquid model is able of describing both shear thickening and shear thinning procedure. The remarkable discussions with respect to Carreau liquid are those of Uhlherr and Chhabra [18] and Bush and Phan-Thein [19] wherein Carreau fluid flow model around the spheres are discussed. After that, Hsu and Yeh [20] analyzed the drag on two coaxial rigid spheres that are moving along the axis of cylinder filled with Carreau liquid. In view of such importance of Carreau nanoliquid, Waqas et al. [21] studied the flow of Carreau nanoliquid subject to heat generation the analysis and modeling for magnetic dipole effect in non-linear thermally radiating. Numerical investigation of momentum and heat transfer of magnetohydrodynamic Carreau nanoliquid via an exponentially stretched plate with internal heat source/sink and radiation is explored by Yousif et al. [22]. Nonlinear and radiation impact on MHD Carreau nanoliquid flow via a radially stretched surface along with zero mass flux at the surface analyzad by Lu et al. [23]. In prespective of its clarity, the remarkable work of current researchers, see few studies [24-35].

The object with stomata is titled as porous medium and is customarily called by some liquid. An excellent number of features including oil production, water flow in reservoirs and catalytic vessels etc. The concept of the liquid flow past a permeable media was first given by a French, Henry Darcy, [36] in 1856. But this approach couldn't be so suitable owing to its limitations of lower porosity and smaller velocity. Afterwards, Philippes Forchheimer [37] modify the momentum equation with the extension of the multiple velocity term into the Darcian velocity to subject the obvious deficiency. This title was later named by Muskat [38] as "Forchheimer term" which is true for high Reynolds number. Mondal and Pal [39] considered the Darcy-Forchheimer model over porous media past the linearly extended surface and deducted that concentration distribution is a diminishing function of electricfield parameter. The hydromagnetic flow of nanofliquid past a Darcy-Forchheimer porous media with the influence of second order boundary condition is determined numerically by Ganesh et al. [40]. Similarly, Alshomrani et al. [41] assumed the 3D Darcy-Forchheimer model along with carbon nanotubes and the homogeneous and the heterogeneous reactions. Theviscous flow of nanoliquids with Darcy-Forchheimer impact via a twisted surface is discussed by Saif et al. [42]. Seth et al. [43] analyzed numerically the flow of carbon nanotubes over a permeable Darcy-Forchheimer media in a rotating body and many therein [44-48].

Chapter 2

Basic preliminaries and laws

This section contains some elementary definitions, basic laws and concepts that are useful in understanding the works in the subsequent chapters.

2.1 Fluid

A substance which consist of particles that contineously distorts when shear stress is applied. Oil, paints, blood, ketchup and water are some examples of fluid.

2.2 Fluid mechanics

The class of mechanics that come with the properties of fluids. It can be classified into two subclasses.

2.2.1 Fluid statics

It investigates the attributes of liquids in a stationary state.

2.2.2 Fluid dynamics

It investigates the attributes of liquids in the state of motion.

2.3 Stress

Stress is the relationship of force F and area A in the deformable body. The SI unit of stress is Nm^{-2} or $kg/m.s^2$. Mathematically,

$$\tau = \frac{F}{A}. \tag{2.1}$$

2.4 Types of stress

It is further divided into two types:

2.4.1 Shear stress

The force that acts on a material parallel to the unit area of the surface is categorized as shear stress.

2.4.2 Normal stress

The force that acts on a material perpendicular to the unit area of the surface is categorized as normal stress.

2.5 Flow

Flow is characterized as a material that distort easily and continuously under the impacts of various kind of forces.

2.6 Types of flow

There are two different ways to describe the flow:

2.6.1 Laminar flow

Flow in which every fluid substance has different layers of fluid and the layer of individual particles do not cross one another.

2.6.2 Turbulent flow

Flow in which every fluid substance has different layers of fluid and the layer of individual particles cross one another.

2.7 Viscosity

Viscosity is an intrinsic fluid property which describes the behavior and motion of the fluid nearest the boundary. It is defined as

$$\mu = \frac{\tau_{yx}}{\frac{du}{dy}}. \tag{2.2}$$

There are two ways to describe the viscosity.

2.7.1 Dynamic viscosity

It is the fluid characteristics that specifies the resistance of fluid versus any deformation with the applied force. Mathematically,

$$\text{viscosity } \ (\mu) = \frac{\text{shear stress}}{\text{gradient of velocity}}. \tag{2.3}$$

2.7.2 Kinematic viscosity

It is the fluid property that specify the ratio of absolute viscosity (μ) to the fluid density (ρ). Mathematically, it is represented by

$$\text{Kinematic viscosity } \ (\nu) = \frac{\mu}{\rho}. \tag{2.4}$$

2.8 Newton viscosity law

The liquids that show the direct and linear relation joining the shear stress and velocity gradient. Mathematically,

$$\tau_{yx} \propto \frac{du}{dy}, \tag{2.5}$$

or

$$\tau_{yx} = \mu \left(\frac{du}{dy} \right), \tag{2.6}$$

here τ_{yx} denotes the shear force, μ the proportionality constant and $\frac{du}{dy}$ the velocity gradient.

2.9 Viscous Fluids

A fluid characterizes as viscous fluid if its viscosity may change or remain uniform due to different type of stresses.

2.9.1 Newtonian fluids

Newtonian liquids are those liquids that follow the Newton's viscosity law or show the direct and linear correspondence joining the shear stress and gradient of velocity. In these liquids force of shear (τ_{yx}) is linearly proportional to the velocity gradient $\left(\frac{du}{dy}\right)$ and μ is constant here. Water, air and glycerin are common examples of Newtonian fluids.

2.10 Non-Newtonian fluids

Fluids that do not satisfy the Newton's viscosity law. Here, nonlinear and direct relation exists joining shear stress and gradient of velocity.

Mathematically,

$$\boldsymbol{\tau}_{yx} \propto \left(\frac{du}{dy} \right)^n, \ n \neq 1, \tag{2.7}$$

or

$$\boldsymbol{\tau}_{yx} = \eta_1 \frac{du}{dy}, \ \eta_1 = k_1 \left(\frac{du}{dy} \right)^{n-1}, \tag{2.8}$$

where η_1, k_1 and n represents apparent viscosity, consistency index and behavior index of flow respectively. For $n = 1$ Eq. (2.8) shows the expression for Newton's viscosity law.

Examples of these liquids are honey, ketchup, paints, blood, tooth paste and polymer solutions etc. These liquids are further divided into three major types *i.e,* (i) differential type (ii) integral type and (iii) rate type.

2.11 Density

Density is termed as mass of a substance per unit volume or ratio between mass and volume. This quantity is utilized to quantify that how much material of a substance present in unit volume.

Mathematically,

$$\rho = \frac{m}{V}, \tag{2.9}$$

where m denotes the mass of the substance and V^* is the volume. The SI unit of density is kg/m^3.

2.12 Pressure

It is defined as a magnitude of force applied perpendicular to the surface per unit area. Mathematical expression for the pressure is given as

$$P = \frac{F}{A}. \tag{2.10}$$

The SI unit of pressure is N/m^2.

2.13 Thermal diffusivity

Thermal diffusivity is a material specific property for explaining the unsteady conductive heat flow. This value describes how speedily a material respond to change in temperature. It is proportion of the thermal conductivity and the multiple of the capacity of specific of heat and density. Mathematically,

$$\alpha = \frac{K}{\rho\,(c_p)}, \tag{2.11}$$

where K shows thermal conductivity, c_p the specific of heat capacity and ρ the density.

2.14 Thermal conductivity

Thermal conductivity is a substance specific property that identifies the heat conduction. It illustrates that how much heat is transferred to the materials. From the Fourier's heat conduction law, it is expressed as a ratio of heat transfered (Q_1) with unit thickness of a substance (l) per unit time and area of surface (A) over the temperature difference (ΔT).

Mathematically,

$$K = \frac{Q_1 l}{A(\Delta T)}.$$

In SI unit it is expressed in kgm/s^3K and its dimension is $(\frac{ML}{T^3\theta})$.

2.15 Porous surface

It is a material which made out of pores, over which fluid or gas can travel through. Few examples are biological tissues, cork and rocks. Sponges, fabrics, ceramics and foams are also gathered for the purpose of porous media.

2.16 Porosity

The measure of spongy space in a porous substance is known as porosity.

2.17 Permeability

It is defined as the strength of a porous substance to allow fluid to travel through it. Those materials which have low porosity are minor permeable while materials having large pores are easily permeated and have high porosity.

2.18 Convective boundary condition

Convective boundary condition are some time called Robin boundary conditions. These kind of condition is usually defined at the wall. Mathematically, this is communicated as:

$$K\left(\frac{\partial T}{\partial r}\right) = \rho\left[\lambda + C_s(T_m - T_0)\right]\upsilon \tag{2.12}$$

where ρ represents the density, λ indicates the latent heat of the liquid, C_s shows the capacity of heat of the solid surface , T_m the melting temperature, T_0 is the solid temperature and υ is the velocity parts along r directions.

2.19 Nanofluid

A liquid that has very small particles in it (called nanometer particles) is said to be Nanofluid. These liquids are formed by the colloidal suspensions of nanoparticles in the conventional liquid. The nanoparticles employed in nanofluids typically are nanotubes, oxides and metals. Most ordinary base fluids are oil and water.

2.20 Carreau fluid model

In this model, the viscous effects are premitted to differ with the deformation rate. This model shows the thickness of a some real liquids, as polymer arrangement and greases, over a very huge scope of qualities of shear rate. The constitutive equation of the this liquid is expressed by:

$$\tau = -pI + \mu(\gamma^{\cdot})A_1, \tag{2.13}$$

$$\mu = \mu_\infty + (\mu_0 - \mu_\infty)\left[1 + (\Gamma\gamma^{\cdot})^2\right]^{\frac{n-1}{2}}, \tag{2.14}$$

Here p is pressure, I the identity tensor, A_1 the first Revlin-Erickson tensor, μ_0 and μ_∞ depicts the zero rate of shear and infinite rate of shear viscosities, Γ material time constant, n the power law index, and the shear rate $\gamma^{\cdot}$ is defined as

$$\gamma^{\cdot} = \sqrt{\frac{1}{2}\Pi}, \qquad \Pi = trace(A_1^2). \tag{2.15}$$

here Π shows the 2^{nd} invariant strain tensor.

It can be noted, the Power-law index shows the liquid behavior and liquid is characterized as shear thinning for $0 < n < 1$, shear thickening for $n > 1$, Newtonian fluid for $n = 1$ and/or

$\Gamma = 0$ and for greater variations of Γ the Power-law model can be obtained.

2.21 Darcy law

It interprets the flow of a liquid through a spongy media. This law was originated and dependent on the consequences of analysis through the water's flow across the beds of sand. It additionally models the scientific basis of liquid permeability needed in the geo sciences.

2.22 Darcy Forchheimer Law

Movements in spongy medium with Reynolds number greater than 10, and in which inertial effects are prominant. So, this inertial term is add on the Darcy's equation and is called as Forchheimer term. This term represents the non-linear influence of the pressure difference versus flow data.

$$\frac{\partial p}{\partial x} = \frac{\mu}{k^*} v_f - \frac{\rho}{k_1} v_f^2, \tag{2.16}$$

where k_1 represents inertial permeability and v_f represents forchheimer velocity.

2.23 Dimensionless numbers

2.23.1 Prandtl number

The relation of momentum diffusivity (ν) to thermal diffusivity (α) is termed as Prandtl number.

Mathematically, it has the following form:

$$\Pr = \frac{\nu}{\alpha} = \frac{\mu c_p}{K}, \tag{2.17}$$

in which μ represents the dynamic viscosity, c_p indicates the specific heat and K stands for thermal conductivity. In transfer of heat, It is control the thicknesses of momentum and boundary layers.

2.23.2 Lewis number

It describes the ratio between kinematic viscosity and Brownian diffusion coefficient. Mathematically,

$$Le = \frac{\nu}{D_B}, \tag{2.18}$$

where $\nu = \mu/\rho$ shows the kinematic viscosity and D_B is the brownian diffusion coefficient.

2.23.3 Thermophoresis parameter

Thermophoresis is a mechanism which is used to prevent the mixing of different particles due to a pressure gradient when they move together or separate the mixture of particles after mixing up. In a cold surface thermophoresis is positive and it is negative for a hot surface.

Mathematically, it can be written as:

$$Nt = \frac{\tau D_T (T_w - T_\infty)}{\upsilon T_\infty}, \tag{2.19}$$

where T_w and T_∞ are the constant temperature and temperature outside the plate, T_w is the constant temperature, D_T is thermophoresis coefficient, τ is the relation of effective heat and heat capacity of the nanoparticles and υ the kinematic viscosity.

2.23.4 Brownian motion parameter

Brownian motion happens due to size of the nanoparticles in a nanofluid. It is a nano scale mechanism that displays the thermal influences of nanofluid. Mathematically,

$$Nb = \frac{\tau D_B (C_\infty)}{\upsilon}, \tag{2.20}$$

where

$$\tau = \frac{(\rho c)_p}{(\rho c)_f}. \tag{2.21}$$

In the above equation τ indicates the relation of effective heat and heat capacity of the nanoparticles and fluid respectively, υ the kinematic viscosity, C_∞ concentration in the free stream and D_B the brownian diffusion coefficient.

2.23.5 Weissenberg number

It is used in the analysis of viscoelastic flow. It is the relationship of the elastic forces to the viscus forces.

$$We = \frac{\text{elastic forces}}{\text{viscous forces}}, \tag{2.22}$$

2.23.6 Peclet number

The Peclet number used in calculations involving convective transfer of heat. It's the proportion of the thermal energy covected to the liquid to the thermal energy conducted within the liquid.

Mathematically,

$$Pe = \frac{dWc}{D_n}, \tag{2.23}$$

where Wc constant maximum cell swimming speed and D_n diffusivity of the microorganism.

2.23.7 Darcy parameter

The Forchheimer number is proposed to identify different flow patterns. This number is determined with the ratio of pressure gradient to the viscous resistance.

Mathematically,

$$Fr = \frac{k^* \rho v \beta^*}{\mu}, \tag{2.24}$$

with β^* non-Darcian coefficient k^* the permeability of the porous media.

2.23.8 Porosity parameter

The ratio between the volume of pores and total volume is described as porosity and this fraction is denoted by porosity parameter.

Mathematically,

$$\lambda = \frac{-vl}{k^* u_0}, \tag{2.25}$$

with k^* the permeability of the porous media, u_0 the reference velocity and l denotes the characteristics length.

2.23.9 Skin friction cofficient

Liquid passing over the surface experiences certain amount of drag that is called as Skin friction. It takes place between the flowing liquid and the solid surface that causes reduction in the rate of flow of fluid. Mathematical form for Skin friction coefficient is given as follows:

$$C_{f_x} = \frac{\tau_{rx}|_{r=R}}{\rho u_w^2}, \tag{2.26}$$

in which τ_{rx} demonstrate shear stress, ρ represents the density and u_w denotes the axial route having velocity.

2.23.10 Nusselt number

The dimensionless number that represents the relation among the convection and conduction heat transfer coefficients at the bondary is known as Nusselt number. Mathematically,

$$Nu_x = \frac{xq_w|r = R}{k\left(T_\infty - T_m\right)}, \tag{2.27}$$

where q_w, ∇T and k represents surface heat flux, temperature difference and thermal conductivity of fluid respectively.

2.23.11 Sherwood number

Sherwood number is a number which is mass transfer rate at the wall.

$$Sh_x = \frac{xq_m}{k \triangle C}, \tag{2.28}$$

where q_w, ∇T and k represents surface heat flux, temperature difference and thermal conductivity of fluid respectively

2.23.12 Reynolds number

The sufficient dimensionless number which is used to recognize that either the flow is laminar or is turbulent. It describes inertial to viscous forces ratio. Mathematically, this number is expressed as:

$$\text{Reynolds number} = \frac{\text{inertial forces}}{\text{viscous forces}}, \tag{2.29}$$

$$\text{Re} = \frac{v \times L}{\nu}. \tag{2.30}$$

Here, v depicts the velocity of fluid, L describe the characteristic length and ν represent kinematic viscosity. Reynolds number are utilized to describe distinct flow behaviours (laminar or turbulent flow) within a similar fluid. Laminar flow arises at small Reynolds number, in which we can note that viscous effects are eminent. Turbulent flow arises at high Reynolds number, where inertial effects are eminent.

2.24 Fundamental laws

The basic laws that are used for the flow description in the subsequential analysis are given below.

2.24.1 Law of mass conservation

Conservation law of mass indicates that the whole mass in any system will remain same. Differential form of law of mass conservation is:

$$\frac{\partial \rho}{\partial t} + (v.\boldsymbol{\nabla})\,\rho + \rho\boldsymbol{\nabla}.\mathbf{v} = 0, \tag{2.31}$$

or

$$\frac{\partial \rho}{\partial t} + \boldsymbol{\nabla}.\,(\rho\mathbf{v}) = 0, \tag{2.32}$$

where ρ shows the density of fluid, $\frac{d}{dt}$ is the substance time derivative and v is the velocity of fluid. It is also known as the equation of continuity. For the steady flow Eq. (2.32) becomes

$$\boldsymbol{\nabla}.\,(\rho\mathbf{v}) = 0, \tag{2.33}$$

and if the fluid is incompressible then Eq. (2.33) implies that

$$\boldsymbol{\nabla}.\mathbf{v} = 0. \tag{2.34}$$

2.24.2 Momentum conservation law

This law describes that the whole linear momentum remains constant of a closed system. Differential form of law of momentum conservation is:

$$\rho \frac{D\mathbf{v}}{Dt} = \text{div}\, \boldsymbol{\tau} + \rho \mathbf{b}. \tag{2.35}$$

In Eq. (2.35) left side represents an internal force, 1^{st} term on right side for the surface force and 2^{nd} term the body force, where b stands for force of body and $\boldsymbol{\tau}$ shows the Cauchy stress tensor for incompressible viscuss fluids.

$$\tau = -P(I) + \mu A_1, \tag{2.36}$$

where

$$A_1 = \text{grad}\, v + (\text{grad}\, v)^t\,,$$

in which P is the pressure, A_1 is the first Rilvin-Erickson tensor, μ the dynamic viscosity and I the identity tensor.

2.24.3 Energy conservation law

This law depicts that the whole energy is conserved in the whole system. Conservation of energy law is also known as energy equation. For nanofluids, it is given by:

$$\rho_f c_f \frac{DT}{Dt} = \tau . L^* + K \nabla^2 T + \rho_p c_p \left(D_B \nabla C . \nabla T + \frac{D_T}{T_\infty} \nabla T . \nabla T \right), \tag{2.37}$$

in which ρ_f represents the base fluid density, c_f stands for specific heat of base fluid, τ the stress tensor, L^* for the strain tensor, ρ_p denotes the density of nanoparticles, D_B denotes the Brownian diffusivity, D_T represents the coefficient of thermophoretic diffusion, K denotes the thermal conductivity and T for temperature.

2.24.4 Law of conservation of concentration

For nanoparticles, the volume fraction equation is

$$\frac{\partial C}{\partial t} = -\frac{1}{\rho_p}\boldsymbol{\nabla}.\mathbf{j}_p, \tag{2.38}$$

or

$$\frac{\partial C}{\partial t} = \mathbf{D}_B\boldsymbol{\nabla}^2\mathbf{C} \ + \mathbf{D}_T\frac{\boldsymbol{\nabla}^2 T}{T_\infty}. \tag{2.39}$$

Here, D_B, C, T and D_T stands for Brownian diffusivity, nanoparticles concentrations, temperature and thermophoretic coefficients respectively.

2.25 Magnetohydrodynamics

The word magnetohydrodynamics (MHD) is the combination of three basic words which are, magneto mean magnetic, hydro mean liquid and dynamics refer to the motion of an objects by the forces. MHD describes the magnetic effects of electrically conducting fluids. Maxwell equations have an important role in MHD studies.

2.26 Heat flow mechanism

Heat is a type of energy that travels from hotter to colder region. Heat transfer process happen between two bodies which are put at various temperatures. The dispersion of heat happens by means of three main mechanisms.

2.26.1 Conduction

A phenomenon in which heat moves from warmer to cooler areas in liquids and solids because of the collisions of free electrons and molecules is called conduction. The process is generally carried out by the heat transfer in material molecule by molecule.

Mathematically,

$$\frac{q}{A} = k\left(\frac{T_1 - T_2}{X_1 - X_2}\right) = k\frac{\triangle T}{\triangle X}, \tag{2.40}$$

where

$$q = -kA\frac{dT}{dx}, \tag{2.41}$$

in which q represents the heat fow, A the area of the surface, K the thermal conductivity, T_1 temperature is greater than, T_2. $\frac{dT}{dx}$ denotes the temperature gradient and minus sign indicates that heat is conducted from higher to lower temperature.

2.26.2 Radiation

The process of heat transfer without any medium is called radiation. The transfer of heat is merely due to the emission of electromagnetic waves. Combined effects of convection and radiation play significant role when heat transfer is considered in the liquids and gases. This phenomenon plays vital role in heat transfer in vaccum.

Mathematically,

$$q = e\sigma^{*}A\left(\triangle T\right)^{4}, \tag{2.42}$$

where q denotes the heat transfer, e for emissivity of the system, σ^{*} for Stephen-Boltzmann's constant, A for area and $(\triangle T)^{4}$ for the temperature difference between two systems of fourth power.

2.26.3 Convection

Mechanism where by heat fows from hot to cold area of liquids or gases due to the movement of molecules is said to be convection.

Mathematically,

$$q = hA\left(T_s - T_{\infty}\right), \tag{2.43}$$

where h is the coefficient heat transfer (convective), T_s for system temperature, A for area and T_{∞} for the ambient temperature.

Chapter 3

Characteristics of melting heat transfer during flow of Carreau fluid induced by a stretching cylinder

In this chapter, the properties of transfer of melting heat in the existence of Carreau liquid flow generated via a stretched cylinder is discussed. Additionally, the melting boundary condition is also considered. The requisite boundary layer equations are transformed within non-linear ordinary differential equations (ODEs) after applying appropriate similarity transformations. The obtained system of linear equations is addressed through built-in function of MATLAB bvp4c scheme. The outcomes of the prominent parameters against involved profiles are portrayed and conversed in the light of their physical importance.

3.1 Mathematical modeling:

Consider an incompressible and axisymmetric transfer of Carreau liquid via a stretched cylinder. The axis of cylinder is on the x-axis while the r-axis is in the radial direction. The surface of stretching cylinder has the velocity $u_w = U_0\,(x/l)$. Moreover, on the flow situation, we supposed the impacts of the melting heat transfer. Here, we consider that T_m is the temperature of melting surface, however, T_∞ is the free stream temperature, such that $T_m < T_\infty$. By letting the origin fixed, two same and opposing forces are applied that the melting surface of cylinder generates a stretching velocity.

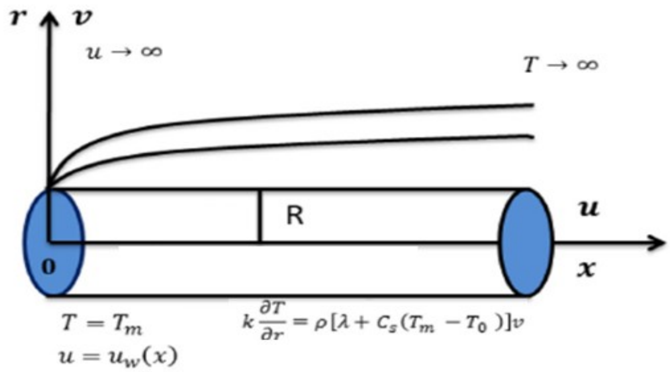

Fig. 3.1 : Geometry of the flow

The governing system representing the given scenario is given as :

$$ru_x + \frac{1}{r}(rv)_r = 0, \tag{3.1}$$

$$uu_x + vu_r = \frac{\nu}{r}u_r\left[1 + \Gamma^2\left(u_r\right)^2\right]^{\frac{n-1}{2}} + \nu u_{rr}\left[1 + \Gamma^2\left(u_r\right)^2\right]^{\frac{n-1}{2}}$$

$$+\nu\left(n-1\right)\Gamma^2\left(u_r\right)^2 u_{rr}\left[1 + \Gamma^2\left(u_r\right)^2\right]^{\frac{n-3}{2}}, \tag{3.2}$$

$$vT_r + uT_x = \frac{k}{\rho c_p}\left(T_{rr} + \frac{1}{r}T_r\right), \tag{3.3}$$

with appropriate boundary conditions

$$u = u_w = \frac{U_0 x}{l},\ T = T_m,$$

$$-K\frac{\partial T}{\partial r} = \rho\left[\lambda + C_s(T_m - T_0\ )\right]v \quad \text{at} \quad r = R,$$

$$u \to 0,\ T \to T_\infty, \quad \text{as} \quad r \to \infty. \tag{3.4}$$

Non dimensionl form of mathematical model is acquired by using following transformations:

$$\eta = \sqrt{\frac{u_w}{vx}}\left(\frac{r^2 - R^2}{2R}\right), \quad \theta\left(\eta\right) = \frac{T - T_m}{T_\infty - T_m},$$

$$u=\frac{U_0x}{l}f'(\eta)\ ,\ v=-\frac{R}{r}\sqrt{\frac{U_0v}{l}}f(\eta)\,. \tag{3.5}$$

Here, satisfaction of Eq. (3.1) is inevitable. However, Eqs. (3.2) to (3.4) take the form:

$$(1+2\gamma\eta)\left\{1+n\,We^2(f'')^2\right\}\left\{1+We^2(f'')^2\right\}^{\frac{n-3}{2}}f''+ff''-\left(f'\right)^2$$

$$+\left[2\gamma f''+\gamma(n+1)\,We^2\left(f''\right)^3\right]\left\{1+We^2\left(f''\right)^2\right\}^{\frac{n-3}{2}}=0, \tag{3.6}$$

$$(1+2\gamma\eta)\,\theta''+2\gamma\theta'+\Pr f\theta'=0, \tag{3.7}$$

$$\theta=0,\quad f'=1,\ \Pr f+M\theta'=0\ \text{ at }\eta=0,$$

$$f'\to 0,\ \theta\to 1,\quad\text{as }\eta\to\infty. \tag{3.8}$$

The values of above mentioned parameters are:

$$We=\sqrt{\frac{b^3x^2r^2\Gamma^2}{l^3R^2v}},\ \gamma^2=\frac{lv}{R^2U_0},\ M=\frac{c_p(T_\infty-T_m)}{\lambda+C_s(T_m-T_0)},\ \Pr=\frac{\mu c_p}{k}, \tag{3.9}$$

The dimensional form of Nussselt number and Skin friction are given by:

$$Nu_x=\frac{x}{k\,(T_\infty-T_m)}q_w\,|_{r=R},\ C_{f_x}=\frac{\tau_{rx}\,|_{r=R}}{\rho u_w^2}, \tag{3.10}$$

Substituting the usual similarity transformation, we get the dimensionless form of Nu_x and C_{f_x} as:

$$\mathrm{Re}^{-\frac{1}{2}}\,Nu_x=-\theta'(0),\ \mathrm{Re}^{-\frac{1}{2}}\,C_{f_x}=f''(0)\left[1+We^2\left\{f''(0)\right\}^2\right]^{\frac{n-1}{2}}, \tag{3.11}$$

where $\mathrm{Re}_x=U_wx/v$ shows the Reynolds number.

3.2 Results and deliberation

The current segment elucidates the impact of numerous parameters *i.e;* melting heat parameter M, parameter of curvature γ, Prandtl number Pr and Weissenberg number We on velocity and temperature profiles. We fixed various flow parameters values as $M = 1.2$, $We = 3.0$, $\Pr = 7.5$, $\gamma = 0.2$, $n = 1.0$. Fig. 3.2 depicts the variations of a dimensionless velocity field versus η for distinct variations of the melting heat parameter M. It indicates, the velocity field rises with the increment of M and the far field boundary conditions are satisfied accordingly. An increment in M will enhance the intensity of melting and as a outcome more heat transfers from the heated liquid to the melting surface. Due to this, more convection flow happens, that automatically enhances the liquid's velocity. The analysis of curvature parameter γ on the velocity profile is drawn in Fig. 3.3. It depicts that for an enhancing variations of curvature parameter γ leads to a greater velocity profile $f'(\eta)$. As the large variations of γ tends to lower the cylinder radius. Hence, low resistance is allowed by the surface and consequently the fluid's velocity rises. The behavior of Pr on the velocity field $f'(\eta)$ is drawn in Fig. 3.4. It is observed that for more variations of Pr velocity profile shows decreasing behavior. As Pr is the relationship of momentum to thermal diffusivity. Increment in Pr tends to downs thermal diffusivity and stronger momentum diffusivity. Fig. 3.5 defines for the greater variations of the curvature parameter γ causes to decrease the liquid's temperature. To the figure we can see that boundary layer be converted to more thick for growing variations of the curvature parameter. Furthermore, the characteristics of melting heat parameter heat M on the profile temperature is illustrated in Fig. 3.6. As the temperature field is decreased by the enhancing values of melting heat parameter M. These results make relation practically, as the melting procedure is used to applying in the act a blowing boundary condition at the stretched surface. Due to this logic, higher melting heat with enhancing M, leads to thick the boundary layer. The change among liquid initial temperature and temperature of the melting surface get increased by enhancing the variations of melting parameter, that causes a decrement in the fluid temperature. The behavior of Pr on the dimensionless temperature field is defined in Fig. 3.7. It is seen that in the existence of melting procedure the liquid's temperature decrease with increasing variations of Pr. The change of the Weissenberg number We on $\theta(\eta)$ is analyzed in Fig. 3.8. It is obvious that the greater variations of the We significantly lowers the temperature profile. But an opposite pattern is measured for the thickness of boundary layer. Moreover, the curves are very near to one another for the flow via a stretched cylinder. Moreover, Table 3.1 illucidates the values of various physical parameters *i.e,* Skin friction coefficient and Nusselt number for the distinct numerical variations of the rising limitations. The C_{f_x} is decreased by the greater values of We, while a different behaviour can observed for the variations of Power law index n. It can be judged that the Nusselt number is an enhancing parameter of Power law index n while an opposite behavior is seen for We.

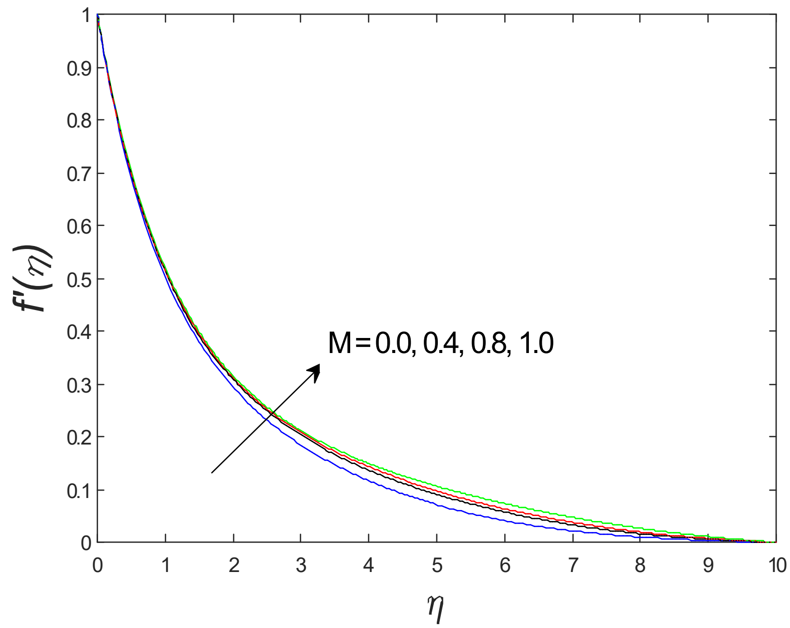

Fig. 3.2 : Change of M on $f'(\eta)$

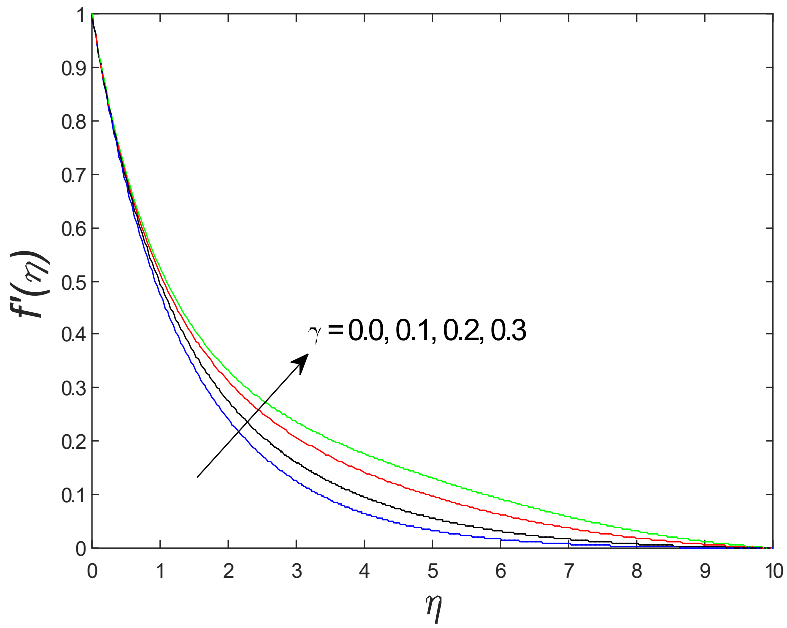

Fig. 3.3 : Change of γ on $f'(\eta)$

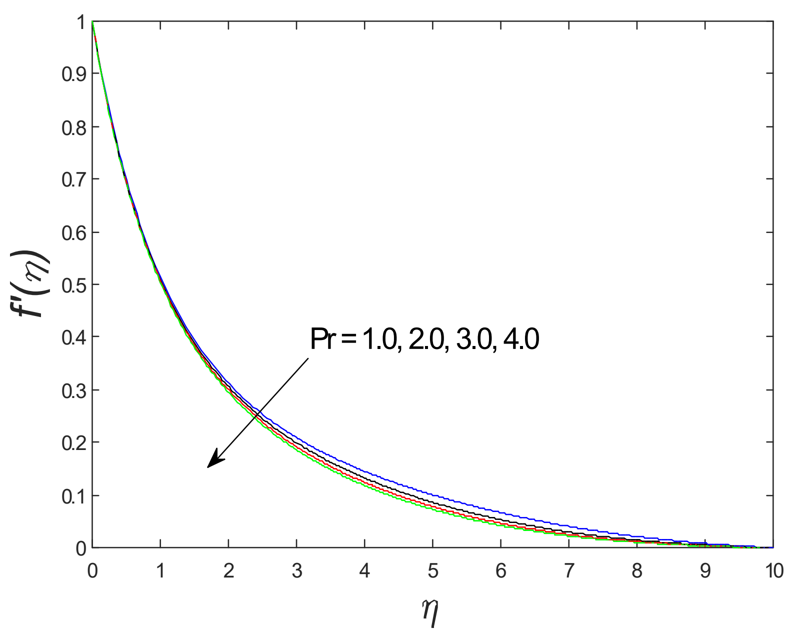

Fig. 3.4 : Change of Pr on $f'(\eta)$

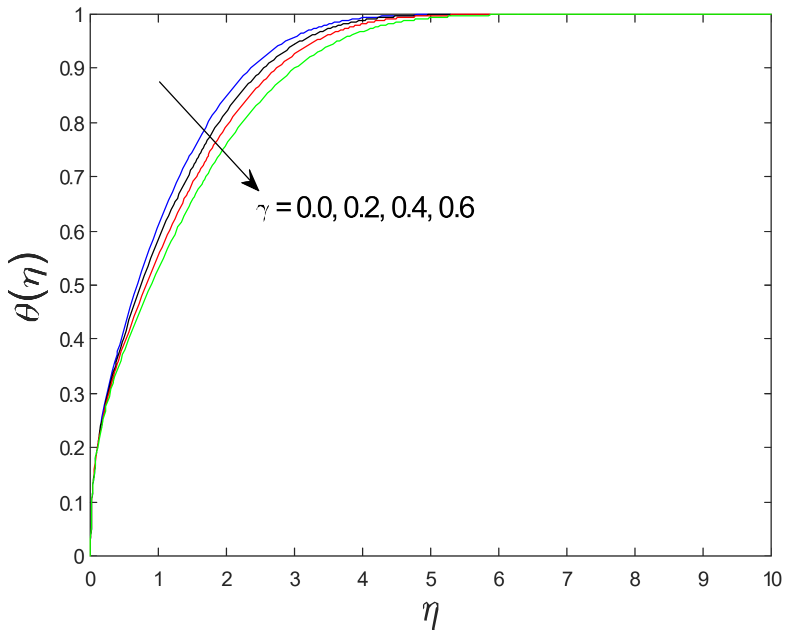

Fig. 3.5 : Change of γ on $\theta(\eta)$

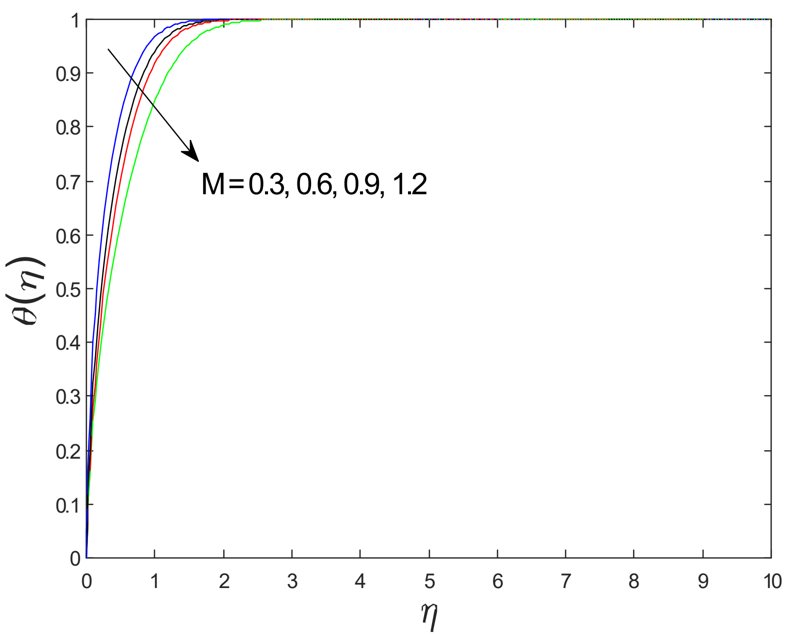

Fig. 3.6 : Change of M on $\theta(\eta)$

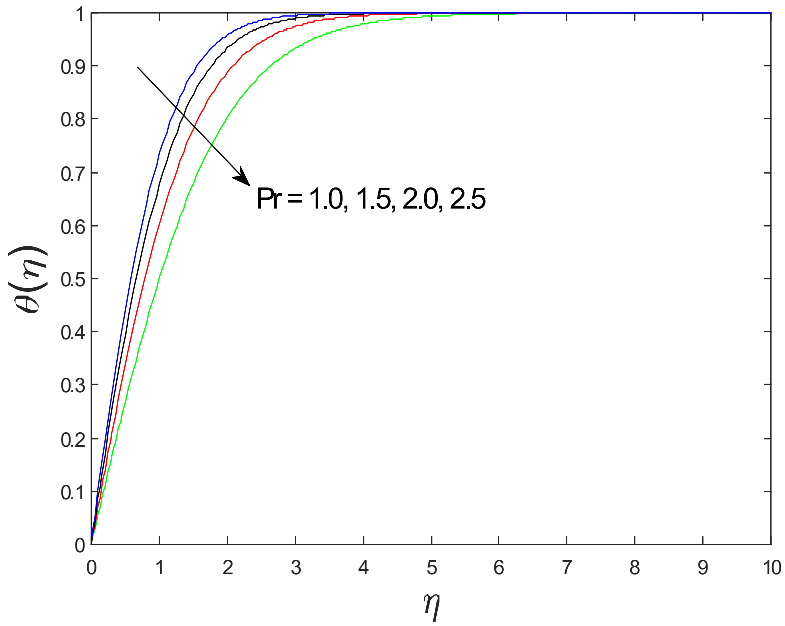

Fig. 3.7 : Change of Pr on $\theta(\eta)$

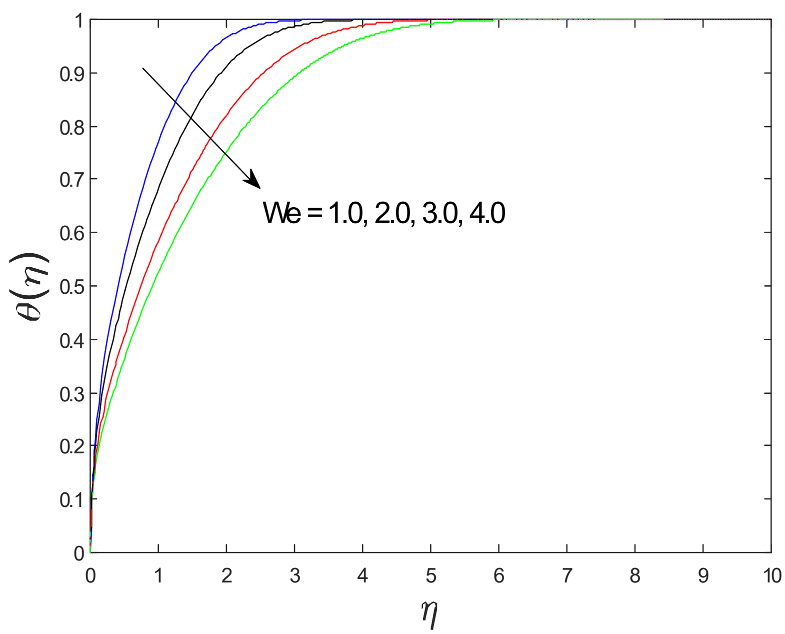

Fig. 3.8 : Change of We on $\theta(\eta)$

Table 3.1 : Variations of C_{f_x} and N_{u_x} for involved parameters.

γ	M	n	We	Pr	$-\mathrm{Re}^{-\frac{1}{2}}\,C_{f_x}$	$-\mathrm{Re}^{-\frac{1}{2}}\,N_{u_x}$
0.3	1.5	1.8	0.6	1.5	1.29245	0.46866
0.4					1.31846	0.49269
0.5					1.34246	0.51365
	0.3				1.49324	0.64794
	0.6				1.42635	0.58979
	0.9				1.37294	0.54220
		0.5			1.51354	0.46741
		1.0			1.51612	0.46895
		1.5			1.51234	0.47024
			0.2		1.30238	0.42558
			0.4		1.11362	0.42510
			0.6		1.02485	0.41698
				1.0	1.40959	0.39990
				1.5	1.44691	0.46866
				2.0	1.46782	0.52892

Chapter 4

Melting heat transfer in the flow of Carreau nanofluid past a stretching cylinder in a Darcy-Farchheimer porous medium

In this chapter, the transfer of melting heat in the flow of Carreau nanoliquid via a stretched cylinder is examined. Moreover, the phenomenon of flow is conducted in the existence of Darcy-Farchheimer porous medium. The nanofluid flow is also discussed in the existence of gyrotactic microorganisms. The governing equations of boundary layer are transformed into non-linear ODEs after applying appropriate similarity transformation. The resulting system of linear equations is addressed by bvp4c built-in function of MATLAB scheme. The outcomes of the prominent parameters versus emerging profiles are portrayed and conversed in the light of their physical significance.

4.1 Mathematical modeling:

Here, we consider an incompressible and axisymmetric transfer of Carreau nanoliquid flow over a stretched cylinder. We consider that T_m is the temperature of melting surface, however, T_∞

is the free stream temperature, such that $T_m < T_\infty$. The surface of stretching cylinder has the velocity $u_w = U_0\,(x/l)$. Moreover, on the flow situation we supposed the impacts of the melting heat transfer. By letting the origin fixed, two same and opposing forces are applied that the melting surface of cylinder generates a stretching velocity. (See Fig. 4.1)

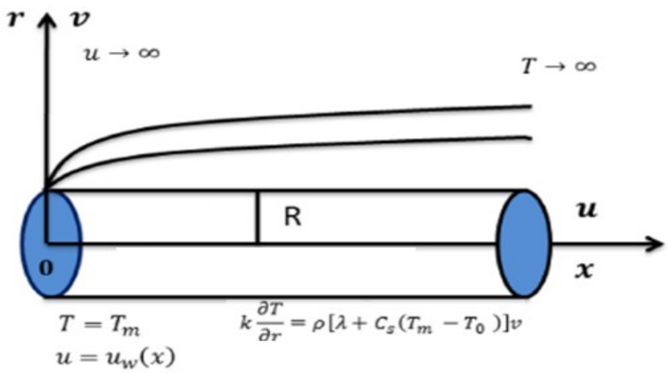

Fig. 4.1 : Geometry of the flow

The resulting boundary layer equations defining the depicted scenario are given as:

$$ru_x + \frac{1}{r}(rv)_r = 0, \tag{4.1}$$

$$uu_x + vu_r = \frac{\nu}{r}u_r\left[1 + \Gamma^2\left(u_r\right)^2\right]^{\frac{n-1}{2}} + \nu u_{rr}\left[1 + \Gamma^2\left(u_r\right)^2\right]^{\frac{n-1}{2}}$$

$$+\nu\left(n-1\right)\Gamma^2\left(u_r\right)^2 u_{rr}\left[1 + \Gamma^2\left(u_r\right)^2\right]^{\frac{n-3}{2}} - \frac{\nu}{k^*}u - Fu^2, \tag{4.2}$$

$$vT_r + uT_x = \frac{k}{\rho c_p}\left(T_{rr} + \frac{1}{r}T_r\right) + \tau\left(D_B C_r T_r + \frac{D_T}{T_\infty}\left(T_r\right)^2\right), \tag{4.3}$$

$$uC_x + vC_r = D_B(C_{rr} + \frac{1}{r}C_r) + \frac{D_T}{T_\infty}(T_{rr} + \frac{1}{r}T_r), \tag{4.4}$$

$$un_x + vn_r = D_n\left(n_{rr} + \frac{1}{r}n_r\right) - \frac{dW_c}{C_w - C_\infty}\left(n_r C_r + nC_{rr}\right). \tag{4.5}$$

with suitable boundary conditions

$$u = u_w = \frac{U_0 x}{l},\ T = T_w,\ C = C_w,\ n = n_w \ \text{ at } r = R,$$

$$-K\frac{\partial T}{\partial r} = \rho\left[\lambda + C_s(T_m - T_0\ )\right]v \ \text{ at } \ r = R,$$

$$u \to 0,\ T \to T_\infty,\ C \to C_\infty,\ n \to n_\infty \ \text{ as } \quad r \to \infty. \tag{4.6}$$

Non dimensionl form of above mathematical flow model is obtained by using following transformations:

$$\eta = \sqrt{\frac{u_w}{vx}}\left(\frac{r^2 - R^2}{2R}\right), \quad \theta(\eta) = \frac{T - T_m}{T_\infty - T_m}\ ,\ \phi(\eta) = \frac{C - C_\infty}{C_w - C_\infty},$$

$$\chi(\eta) = \frac{n - n_\infty}{n_w - n_\infty},\ u = \frac{U_0 x}{l} f'(\eta)\,, \quad v = -\frac{R}{r}\sqrt{\frac{U_0 v}{l}} f(\eta)\,. \tag{4.7}$$

Here, satisfaction of Eq. (4.1) is inevitable. However, Eqs. (4.2) – (4.5) take the form:

$$(1 + 2\gamma\eta)\left\{1 + n\,We^2(f'')^2\right\}\left\{1 + We^2(f'')^2\right\}^{\frac{n-3}{2}} f'' + ff'' - \left(f'\right)^2$$

$$+\left[2\gamma f'' + \gamma(n+1)\,We^2\left(f''\right)^3\right]\left\{1 + We^2\left(f''\right)^2\right\}^{\frac{n-3}{2}} - \beta f' - F_r\left(f'\right)^2 = 0, \tag{4.8}$$

$$(1 + 2\gamma\eta)\,\theta'' + 2\gamma\theta' + \Pr f\theta' + (1 + 2\gamma\eta)\Pr\left(Nb\theta'\phi' + Nt\theta'^2\right) = 0, \tag{4.9}$$

$$(1 + 2\gamma\eta)\,\phi'' + 2\gamma\phi' + Lef\phi' + \frac{Nt}{Nb}\left((1 + 2\gamma\eta)\,\theta'' + 2\gamma\theta'\right) = 0, \tag{4.10}$$

$$(1 + 2\gamma\eta)\,\chi'' + 2\gamma\chi' + Lb\Pr f\chi'$$

$$-Pe\begin{pmatrix} (1 + 2\gamma\eta)\,\chi'\phi' + \gamma\chi\phi' + (1 + 2\gamma\eta)\,\chi\phi'' \\ +\sigma\gamma\phi' + \sigma\,(1 + 2\gamma\eta)\,\phi'' \end{pmatrix} = 0. \tag{4.11}$$

$$\theta = \phi = \chi = 1, \quad f' = 1,\ \ \Pr f + M\theta' = 0 \ \text{ at } \eta = 0,$$

$$f' \to 0,\ \chi \to 0, \quad \theta \to 0, \quad \phi \to 0 \ \text{ as } \eta \to \infty. \tag{4.12}$$

The variations of above mentioned parameters are:

$$We = \sqrt{\frac{b^3 x^2 r^2 \Gamma^2}{l^3 R^2 v}},\ \gamma^2 = \frac{lv}{R^2 U_0},\ M = \frac{c_p(T_\infty - T_m)}{\lambda + C_s(T_{m-}T_0)},\ \Pr = \frac{\mu c_p}{k},$$

$$\nu = \frac{\mu_0}{\rho}, \quad \sigma = \frac{n_\infty}{n_w - n_\infty}, \quad Nb = \frac{\tau D_B C_\infty}{\nu}, \quad Nt = \frac{\tau D_T \left(T_\infty - T_m\right)}{\nu T_\infty},$$

$$Le = \frac{\nu}{D_b}, \quad Lb = \frac{\alpha}{D_n}, \quad Pe = \left(\frac{dw_c}{D_n}\right). \tag{4.13}$$

The dimensional form of Nussselt and Sherwood numbers, Skin friction and the Motile microorganism density number are given by:

$$Nu_x = \frac{xq_w|r = R}{k\left(T_\infty - T_m\right)}, \; C_{f_x} = \frac{\tau_{rx}|r = R}{\rho u_w^2},$$

$$Sh_x = \frac{xq_m}{D_B \triangle C}, \quad Nn_x = \frac{xq_n}{D_n \triangle n}. \tag{4.14}$$

Substituting the usual similarity transformation, we get the dimensionless form of Nu_x, C_{f_x}, Sh_x and Nn_x

$$\mathrm{Re}^{-\frac{1}{2}} Nu_x = -\theta^{'}(0), \;\; \mathrm{Re}^{-\frac{1}{2}} C_{f_x} = f^{''}(0)\left[1 + We^2\left\{f^{''}(0)\right\}^2\right]^{\frac{n-1}{2}},$$

$$\mathrm{Re}^{-\frac{1}{2}} Sh_x = -\phi'\left(0\right), \quad \mathrm{Re}^{-\frac{1}{2}} Nn_x = -\chi'\left(0\right). \tag{4.15}$$

here $\mathrm{Re}_x = U_w x/v$ shows the Reynold number.

4.2 Results and deliberation

The purpose of this portion is to draw the impact of emerging parameters on velocity, temperature, concentration and gyrotactic microorganism distributions. Various parameters like melting heat parameter M, Prandtl number Pr, Weissenberg number We, Darcy parameter Fr, porosity parameter λ, parameter of Brownian motion Nb, parameter of curvature γ, thermophoresis parameter Nt, Lewis number Le, Bioconvection lewis number Lb, Peclet number Pe and Bio- convection parameter σ. We fixed different flow parameters values as $M = 1.2$, $\gamma = 0.2$, $\Pr = 7.5$, $We = 2.0$, $Fr = 0.2$, $\lambda = 0.2$, $Nb = 0.4$, $Nt = 0.6$, $Le = 1.0$, $Pe = 1.2$, $Lb = 0.2$, $\sigma = 1.0$, and $n = 1.0$ are discussed on axial velocity, temperature , nanoparticles concentration and gyrotactic microorganism distributions. Fig. 4.2 displays the velocity field for distinct variations of the melting heat parameter M. The velocity field enhances with the increase of M. It indicates that the velocity field rises with the increment of M and the far field boundary conditions are fulfilled accordingly. An increment in M will enhance the intensity of melting and as a outcome more heat transfer to the heated liquid to the melting surface. Due to this, more convection flow happens, that automatically increases the liquid velocity. The study of the curvature parameter γ on the velocity field is sketched in Fig. 4.3. It shows that the an enhancing variations of curvature parameter γ tends to a greater velocity field. It is detected from the figure that an increment in the parameter of curvature effects an upgrad in the axial velocity profile. The increasing variations of M tends to lower the cylinder's radius. So, lower resistance is given by the surface and consequently the liquids velocity upgrades. Illustration of Darcy parameter Fr on $f'(\eta)$ is displayed in Fig. 4.4. It is examined that for expanding variations of Fr, the decreasing behavior of the velocity distribution is seen. This is because, for the higher values of Fr leads to a resistance in a fluid flow. Fig. 4.5 is drawn to show the behavior of porosity number λ to the velocity distribution $f'(\eta)$. It is explored that the velocity of the liquid is reduced for higher variations of porosity parameter. Usually, the movement of the fluid is hold up due to the presence of porous media and as a outcome it causes in the falloff of fluid velocity. Fig. 4.6 defines for the greater variations of γ lead to decrease the liquid's temperature. It is judged that the thermal boundary layer converted into more thick for increasing variations of the curvature parameter. Furthermore, the characteristics of melting heat parameter M on temperature field is drawn in Fig. 4.7. It is observed that the $\theta(\eta)$ is lowered for the melting heat parameter. The outcome of Pr on $\theta(\eta)$ is drawn in Fig. 4.8. It is judged that in the existence of melting procedure the liquid temperature decrease with increasing variations of Pr. So, it can be judged that for greater variations of Pr temperature field enhances. The presence of the Weissenberg number We on the $\theta(\eta)$ is analyzed in Fig. 4.9. It is seen that the greater variations of the We, significantly lower the temperature profile. But a different pattern is judged for the thermal boundary layer thickness. Fig. 4.10 is sketched to show the change of curvature parameter γ on nanoparticles concentration profile $\phi(\eta)$. It depicts, for an increasing variations of curvature parameter γ leads to a greater nanoparticles concentration distribution $\phi(\eta)$. The decending behavior in concentration distribution $\varphi(\eta)$ of Brownian motion parameter Nb is drawn in Figure 4.11. In the flow of nanofluid, by the appearence of nanoparticles, the Brownian motion happens, and with an enhancement in the Brownian motion parameter Nb the Brownian motion is changed and similarly the boundary layer thickness decreases. Fig.

4.12 indicates the increasing behavior of thermophoresis parameter Nt in concentration field $\varphi(\eta)$. Both the $\phi(\eta)$ and the thickness of thermal layer are increased for rising variations of thermophoresis parameter Nt. Large variations of Nt causes an increment in the thermophoresis force for that leads to go nanoparticles to cold from hotter surfaces and similarly it rises the thickness of thermal layer. Outcomes of Lewis number Le on $\phi(\eta)$ is illustrated in Fig. 4.13. The nanoparticles concentration decreased quickly when we enhance the variations of Le. This decrement in $\phi(\eta)$ is by the change in Brownian diffusion coefficient. Higher Lewis number tends to lower Brownian diffusion coefficient. Figure 4.14 shows the behavior against Peclet number Pe on gyrotactic microorganism profile $\chi(\eta)$. Here, $\chi(\eta)$ is an enhancing function of Pe, that affects to a decrease in the diffusivity of microorganisims. Figure 4.15 sketched to indicate the curves of $\chi(\eta)$ for various terms of bioconvection Lewis number Lb while other variables are fixed. It can be judged that Lb depicts the decreasing behavior for large values of Lb. Figure 4.16 indicates the variations in gyrotactic microorganism profile $\chi(\eta)$ for various variations of bioconvection parameter σ. Large variations of bioconvection parameter causes the reduction in gyrotactic microorganism profile. Figure 4.17 is drawn to analyze the differences in concentration for numerous variations of Pr. Here, it is noticed that the thickness of boundary layer and gyrotactic microorganism profile $\chi(\eta)$ are decending function of Pr. There is a reverse relationship with Prandtl number and thermal diffusivity. An increment in Pr, leads to lower thermal diffusivity that causes to lower the gyrotactic microorganism profile and thermal layer thickness.

Moreover, Table 4.1 illucidates the limitations of various physical parameters *i.e;* Skin friction and Nusselt number for the different numerical variations of the rising parameters. The C_{f_x} is decreased by the greater values of We, while a quite different behaviour can seen for the variations of Power law index n. It can be judged that the Nusselt number is an enhancing parameter of power law index n while an opposite behavior is noted for We.

Table 4.2 indicates the numerical limitations of C_{f_x}, N_{u_x}, Sh_x and N_{n_x} for distinct variations of M, Pr, Nb, Nt and σ. We noted that the variations of Skin friction and Nusselt number enhances with an enhancing variations of melting parameter M, while the reverse change is noted in the case of Sherwood number and density number. Furthermore, the variations of C_{f_x} and Nu_x decresed with the enhancing variations of Prandtl number Pr, and quite different behavior is judged for Sherwood number and density number of motile microorganism. Similarly, for an increasing variations of Brownian motion parameter Nb, the variations of Skin friction lowers while the variations of N_{u_x}, Sh_x and N_{n_x} enhances. It can be noticed that for an enhancing variations of thermophoresis parameter Nt the variations of C_{f_x}, N_{u_x} and N_{n_x} decreases while Sherwood number Sh_x increases. Lastly, it is noted that for an enhancing variations of bio-convection parameter σ, the paarametrs C_{f_x}, N_{u_x} and Sh_x shows the same behavior while the number of density motile microorganism N_{n_x} shows the increasing behavior.

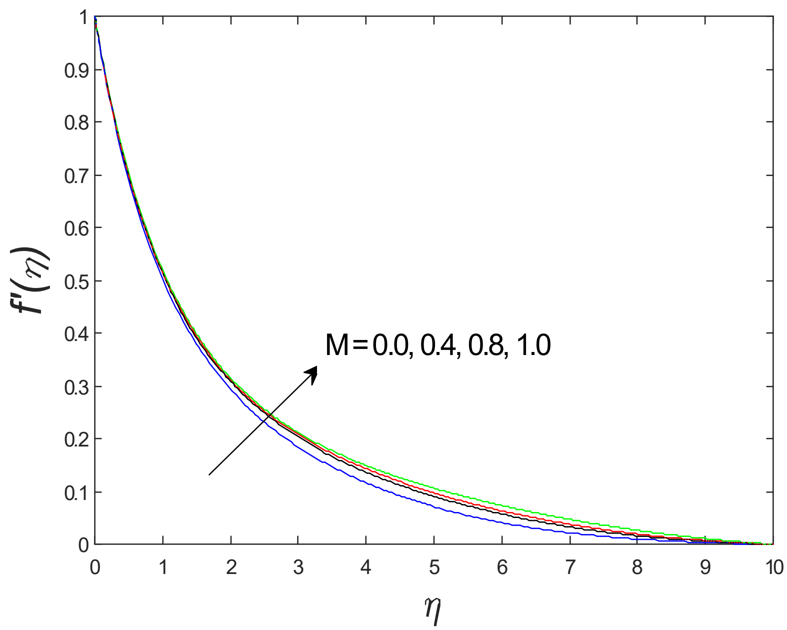

Fig. 4.2 : Change of M on $f^{'}(\eta)$

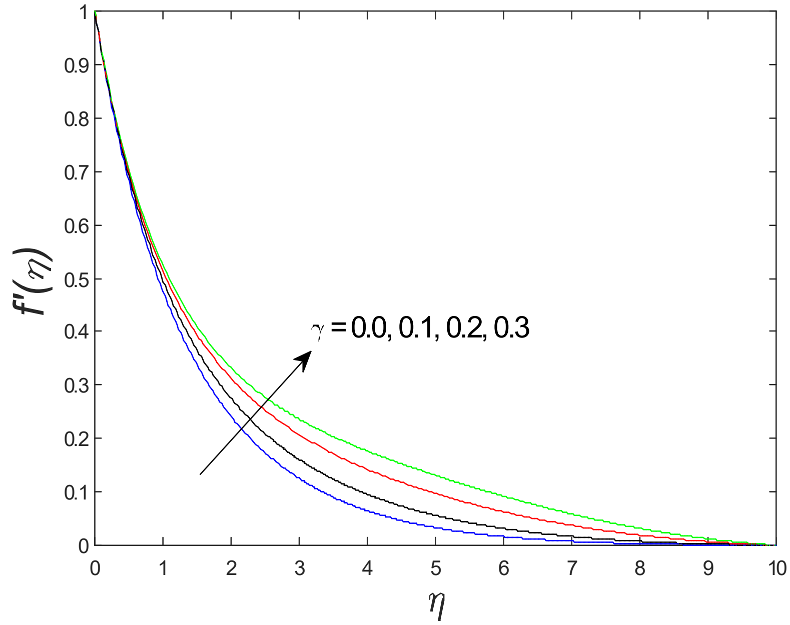

Fig. 4.3 : Change of γ on $f'(\eta)$

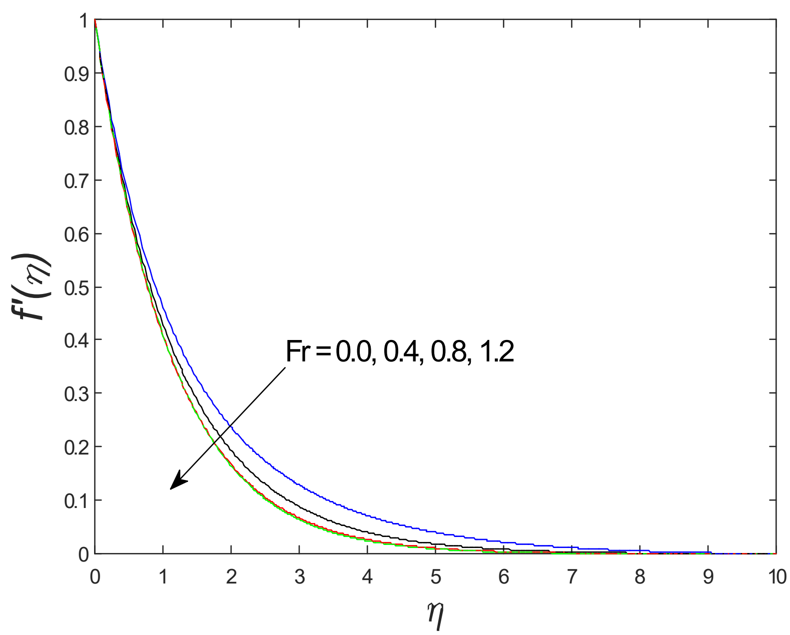

Fig. 4.4 : Change of Fr on $f'(\eta)$

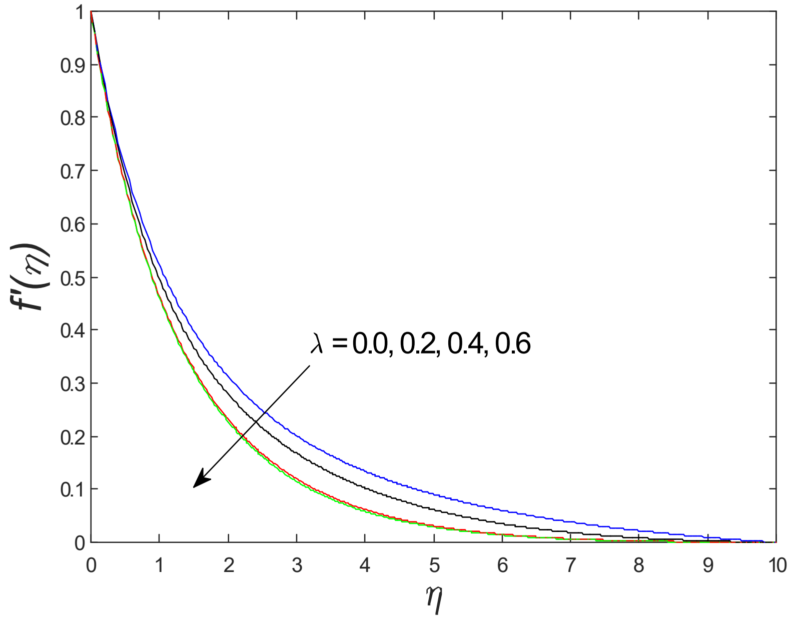

Fig. 4.5 : Change of λ on $f'(\eta)$

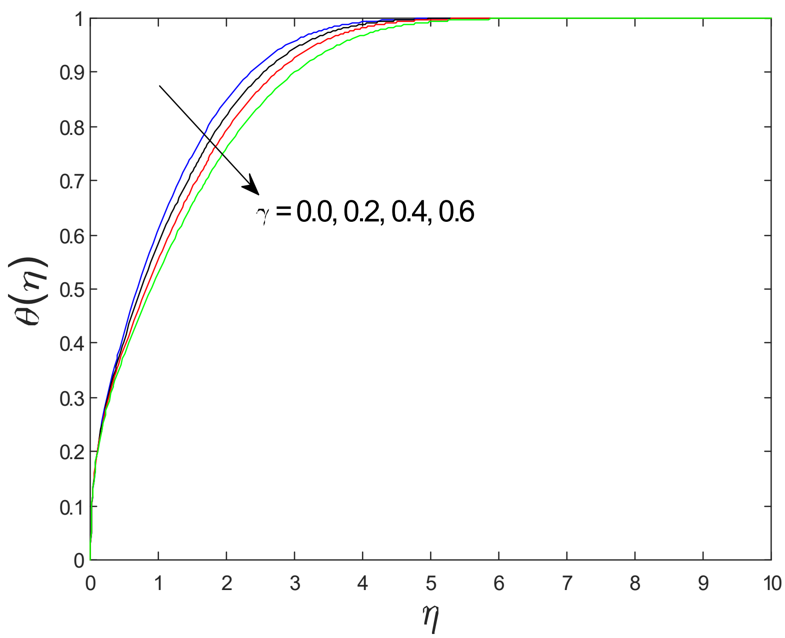

Fig. 4.6 : Change of γ on $\theta(\eta)$

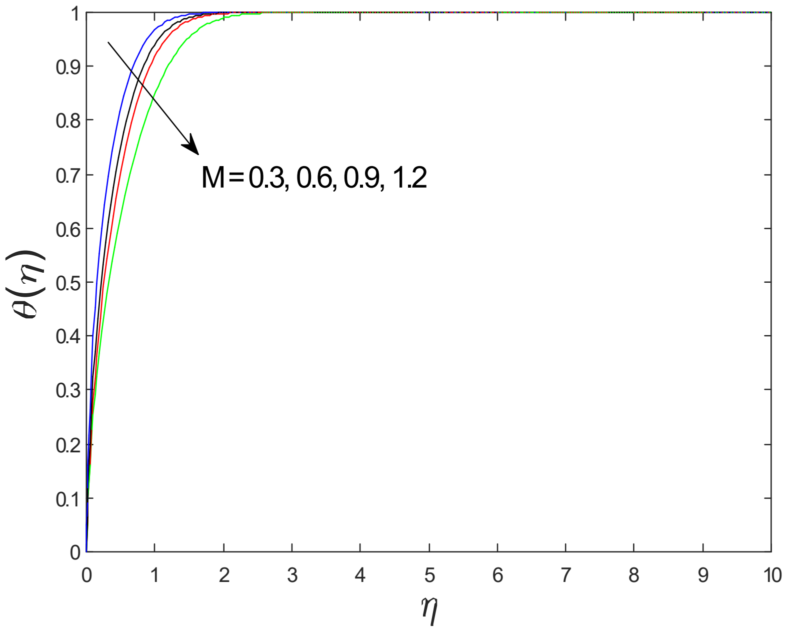

Fig. 4.7 : Change of M on $\theta(\eta)$

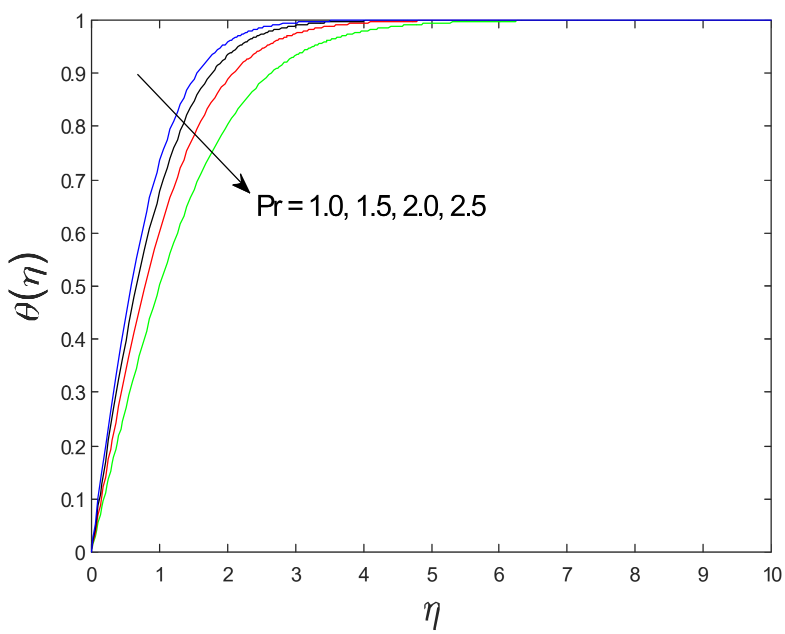

Fig. 4.8 : Change of Pr on $\theta(\eta)$

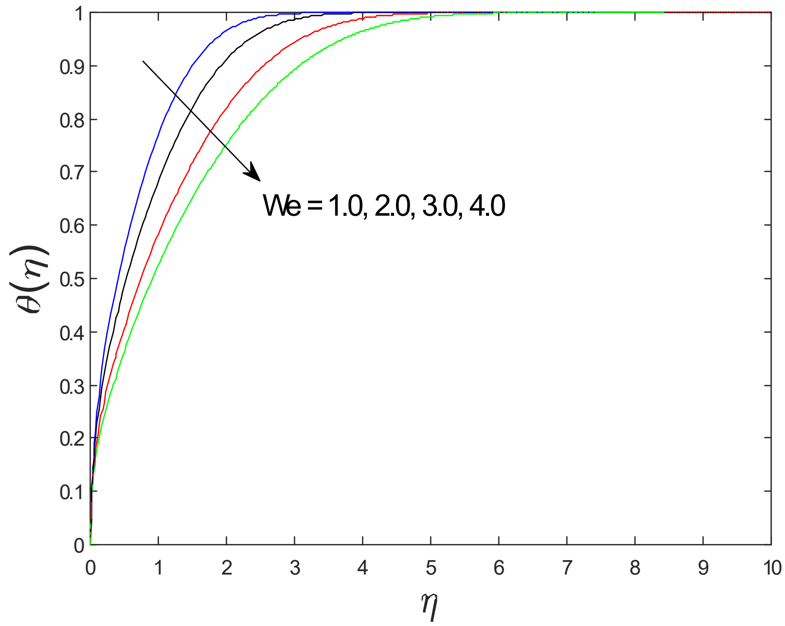

Fig. 4.9 : Change of We on $\theta(\eta)$

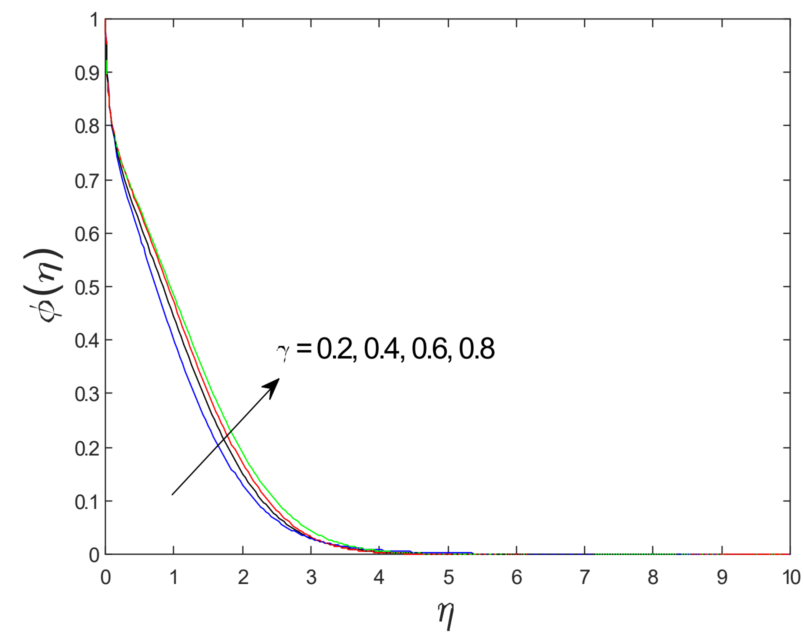

Fig. 4.10 : Change of γ on $\phi(\eta)$

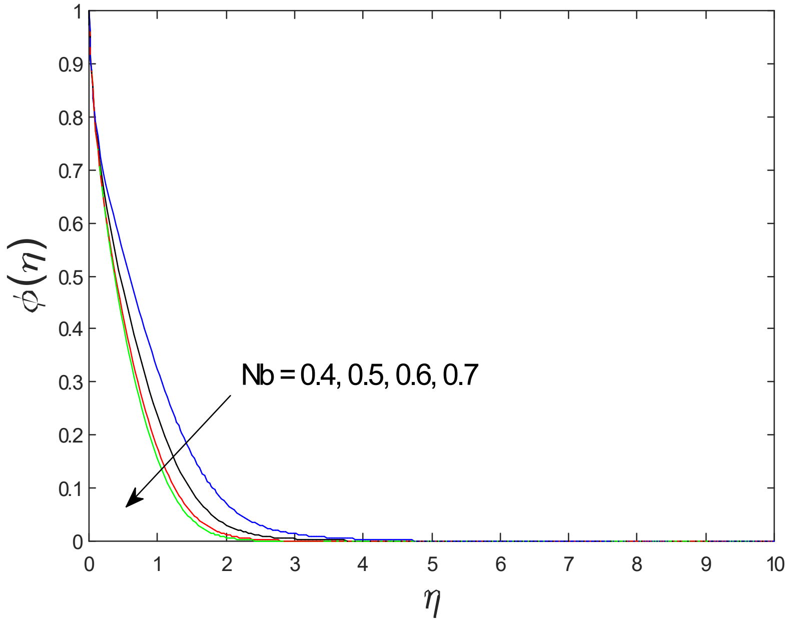

Fig. 4.11 : Change of Nb on $\phi(\eta)$

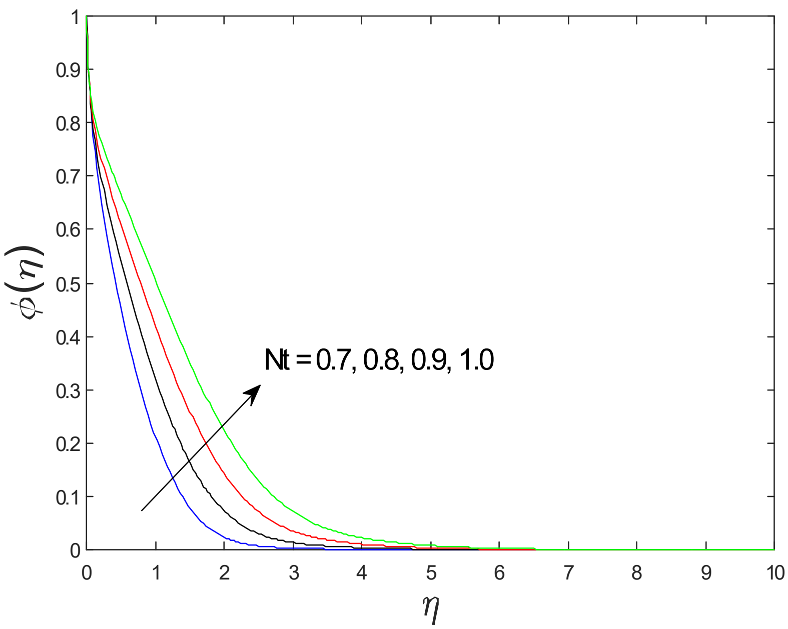

Fig. 4.12 : Change of Nt on $\phi(\eta)$

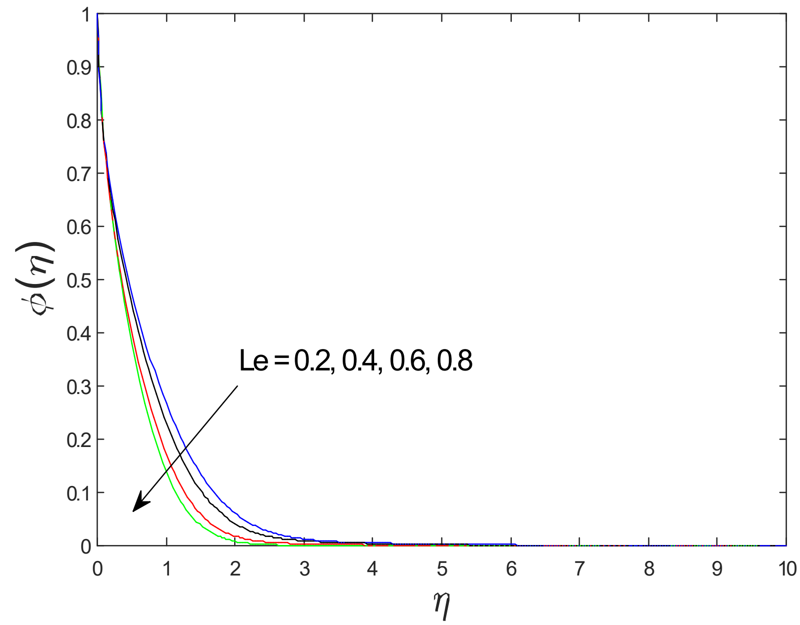

Fig. 4.13 : Change of Le on $\phi(\eta)$

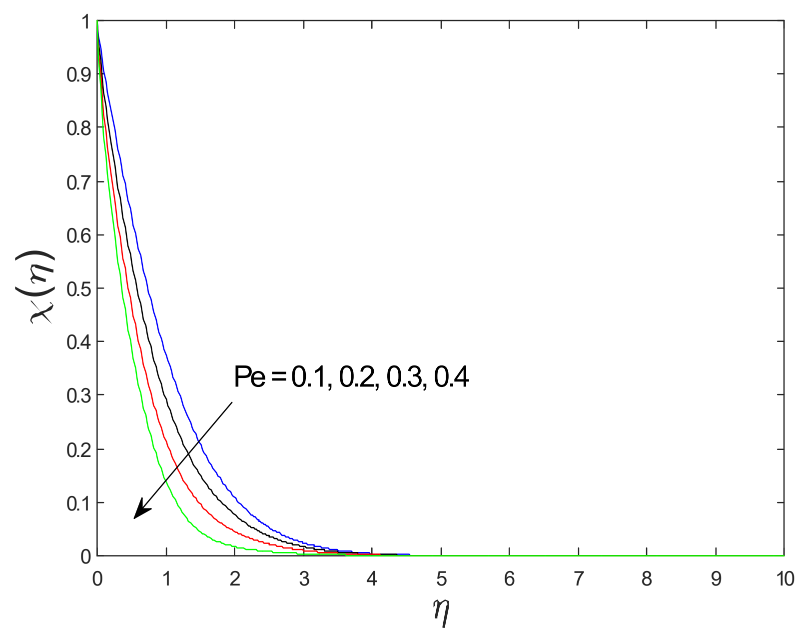

Fig. 4.14 : Change of Pe on $\chi(\eta)$

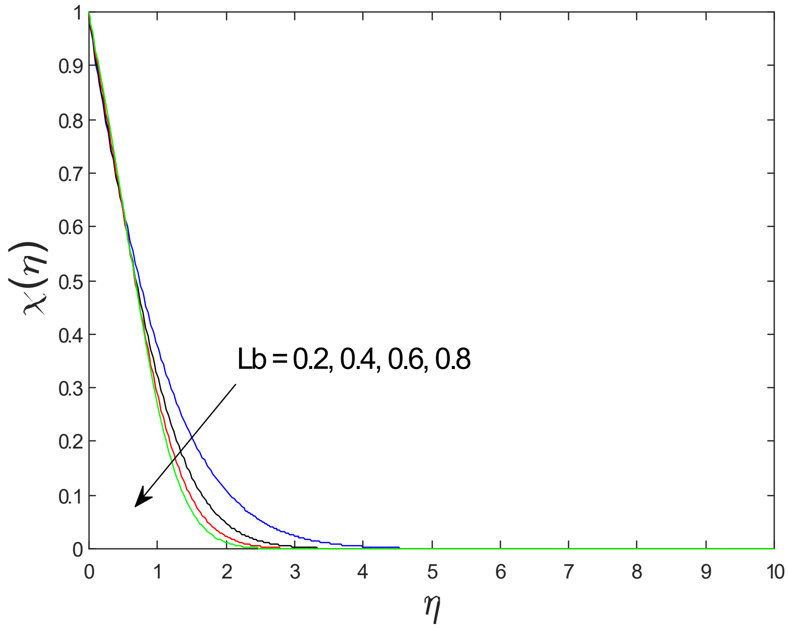

Fig. 4.15 : Change of Lb on $\chi(\eta)$

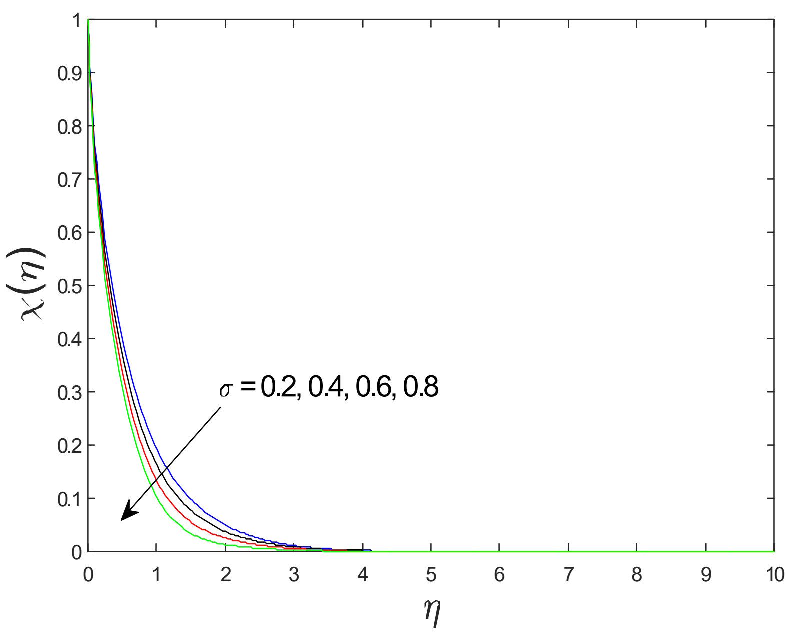

Fig. 4.16 : Change of σ on $\chi(\eta)$

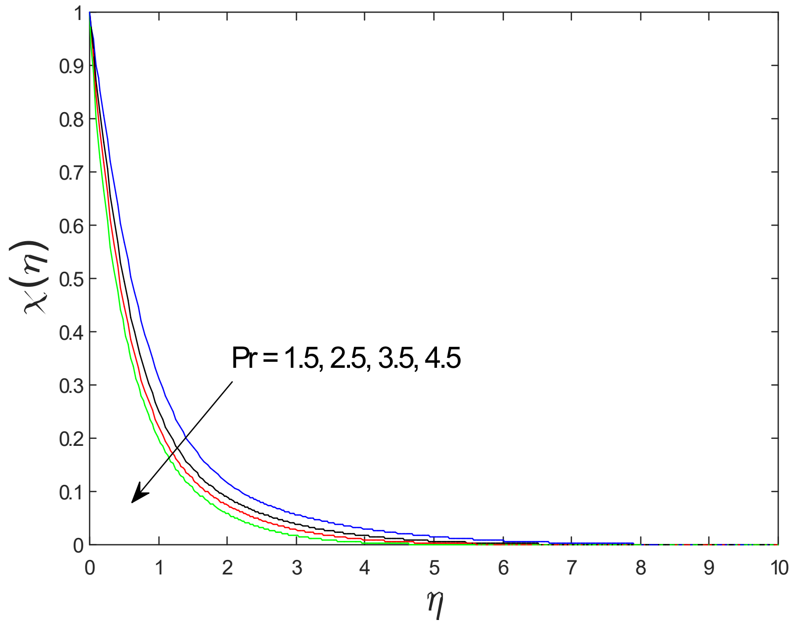

Fig. 4.17 : Change of Pr on $\chi(\eta)$

Table 4.1 : Variations of C_{f_x} and N_{u_x} for involved parameters.

γ	M	n	We	Pr	$-\mathrm{Re}^{-\frac{1}{2}}\, C_{f_x}$	$-\mathrm{Re}^{-\frac{1}{2}}\, N_{u_x}$
0.3	1.5	1.8	0.6	1.5	1.29245	0.46866
0.4					1.31846	0.49269
0.5					1.34246	0.51365
	0.3				1.49324	0.64794
	0.6				1.42635	0.58979
	0.9				1.37294	0.54220
		0.5			1.51354	0.46741
		1.0			1.51612	0.46895
		1.5			1.51234	0.47024
			0.2		1.30238	0.42558
			0.4		1.11362	0.42510
			0.6		1.02485	0.41698
				1.0	1.40959	0.39990
				1.5	1.44691	0.46866
				2.0	1.46782	0.52892

Table 4.2 : Variations of C_{f_x}, N_{u_x}, Sh_x and N_{n_x} for various parameters.

M	Pr	Nb	Nt	σ	$-\mathrm{Re}^{-\frac{1}{2}}\,C_{f_x}$	$-\mathrm{Re}^{-\frac{1}{2}}\,N_{u_x}$	$\mathrm{Re}^{-\frac{1}{2}}\,Sh_x$	$\mathrm{Re}^{-\frac{1}{2}}\,N_{n_x}$
0.3	1.5	1.8	0.6	0.2	1.49324	0.64794	0.70839	0.39341
0.6					1.42635	0.58979	0.64438	0.39058
0.9					1.37294	0.54220	0.59188	0.38855
	1.0				1.40959	0.39990	0.30722	0.38397
	1.5				1.44691	0.46866	0.51061	0.38592
	2.0				1.46782	0.52892	0.55547	0.38871
		0.5			1.24853	0.46866	0.51061	0.38592
		0.6			1.26012	0.44508	0.51352	0.38624
		0.7			1.27173	0.42170	0.51834	0.38656
			0.2		1.21428	0.41180	0.51061	0.38592
			0.5		1.24853	0.46866	0.51352	0.38542
			0.7		1.32625	0.50929	0.51834	0.38446
				0.2	1.31991	0.42618	0.51061	0.38592
				0.4	1.31991	0.42618	0.51061	0.38634
				0.6	0.31991	0.42618	0.51061	0.38675

Chapter 5

Concluding remarks and Future work

In this thesis, two problems have been analyzed where first problem is about review paper and second problem is the extension work. Conclusion of both the problems are as follows:

5.1 Chapter 3

The characteristics of melting heat transfer with convective boundary condition in three-dimensional (3D) Carreau nanofluid flow induced through a stretched cylinder. The extensive findings of this investigation are given below:

- For large variations of melting heat parameter M, the velocity field is greater.
- Larger variations in parameter of curvature γ causes an increment in velocity distribution while temperature profile decreases.
- Enhancing values of Pr shows the decreasing behavior on velocity profile, while quite different result is observed in the case of temperature distribution.
- Temperature profile decreases for greater variations of Weissenberg number We.
- An enhancement in parameter of curvature M tends to decrease the temperature profile.

5.2 Chapter 4

In the current exploration, The transfer of the melting heat in the flow of Carreau nanofluid over a stretched cylinder in the darcy-Farchheimer porous media is studied. Solution of the assumption is addressed by MATLAB scheme of bvp4c built-in function. The significant outcomes of the present investigation are given as:

- Behavior of melting heat parameter M on the velocity and temperature fields are reverse.
- Enhancing variations of Curvature parameter γ will tend to increase the velocity and concentration distributions while lower the temperature distribution.
- Velocity field decreases for enhancing variations of Darcy parameter Fr.
- Porosity number decrease the velocity field.
- Thermophoresis parameter and Brownian motion parameter display the different results on nanoparticles concentration field.
- Peclet number Pe decrease the gyrotactic microorganism distributiion.
- Gyrotactic microorganism profile reduces for large values of bioconvection parameter σ.

5.3 Future work

The current analysis can be extended to the following models as well:

- The fluid flow may be extended to the any other non-Newtonian fluids.
- The Buongiorno nanofluid model may be swapped with Tiwari and Das model.
- Some varied types of base fluids and nano-materials may be used.
- Some different non-Newtonian fluid model may also be considered.
- Boundary conditions may be replaced with convective and zero-mass flux conditions.
- Effect of Hall current and dusty fluid may also be considered.

Bibliography

[1] Sheikholeslami, M., Arabkoohsar, A., & Jafaryar, M. (2020). Impact of a helical-twisting device on the thermal–hydraulic performance of a nanofluid flow through a tube. Journal of Thermal Analysis and Calorimetry, 139(5), 3317-3329.

[2] Ramzan, M., Ullah, N., Chung, J. D., Lu, D., & Farooq, U. (2017). Buoyancy effects on the radiative magneto Micropolar nanofluid flow with double stratification, activation energy and binary chemical reaction. Scientific Reports, 7(1), 1-15.

[3] Yang, L., Huang, J. N., Ji, W., & Mao, M. (2020). Investigations of a new combined application of nanofluids in heat recovery and air purification. Powder Technology, 360, 956-966.

[4] Li, F., Sheikholeslami, M., Dara, R. N., Jafaryar, M., Shafee, A., Nguyen-Thoi, T., & Li, Z. (2020). Numerical study for nanofluid behavior inside a storage finned enclosure involving melting process. Journal of Molecular Liquids, 297, 111939.

[5] Tayebi, T., & Chamkha, A. J. (2020). Entropy generation analysis due to MHD natural convection flow in a cavity occupied with hybrid nanofluid and equipped with a conducting hollow cylinder. Journal of Thermal Analysis and Calorimetry, 139(3), 2165-2179.

[6] Waqas, M., Khan, M. I., Hayat, T., & Alsaedi, A. (2017). Numerical simulation for magneto Carreau nanofluid model with thermal radiation: a revised model. Computer Methods in Applied Mechanics and Engineering, 324, 640-653.

[7] Hsiao, K. L. (2017). To promote radiation electrical MHD activation energy thermal extrusion manufacturing system efficiency by using Carreau-Nanofluid with parameters control method. Energy, 130, 486-499.

[8] Ramzan, M., Bilal, M., Chung, J. D., & Farooq, U. (2016). Mixed convective flow of Maxwell nanofluid past a porous vertical stretched surface–An optimal solution. Results in Physics, 6, 1072-1079.

[9] Khan, M., & Azam, M. (2017). Unsteady heat and mass transfer mechanisms in MHD Carreau nanofluid flow. Journal of Molecular Liquids, 225, 554-562.

[10] Bhatti, M. M., Abbas, T., Rashidi, M. M., & Ali, M. E. S. (2016). Numerical simulation of entropy generation with thermal radiation on MHD Carreau nanofluid towards a shrinking sheet. Entropy, 18(6), 200.

[11] Hussain, T., Hussain, S., & Hayat, T. (2016). Impact of double stratification and magnetic field in mixed convective radiative flow of Maxwell nanofluid. Journal of Molecular Liquids, 220, 870-878.

[12] Yang, L., Du, K., & Zhang, Z. (2020). Heat transfer and flow optimization of a novel sinusoidal minitube filled with non-Newtonian SiC/EG-water nanofluids. International Journal of Mechanical Sciences, 168, 105310.

[13] Tlili, I., Naseer, S., Ramzan, M., Kadry, S., & Nam, Y. (2020). Effects of Chemical Species and Nonlinear Thermal Radiation with 3D Maxwell Nanofluid Flow with Double Stratification—An Analytical Solution. Entropy, 22(4), 453.

[14] Sulochana, C., Ashwinkumar, G. P., & Sandeep, N. (2016). Transpiration effect on stagnation-point flow of a Carreau nanofluid in the presence of thermophoresis and Brownian motion. Alexandria Engineering Journal, 55(2), 1151-1157.

[15] Khan, M. I., Kumar, A., Hayat, T., Waqas, M., & Singh, R. (2019). Entropy generation in flow of Carreau nanofluid. Journal of Molecular Liquids, 278, 677-687.

[16] Hayat, T., Ullah, I., Muhammad, T., Alsaedi, A., & Shehzad, S. A. (2016). Three dimensional flow of Powell–Eyring nanofluid with heat and mass flux boundary conditions. Chinese Physics B, 25(7), 074701.

[17] Ramzan, M., Bilal, M., & Chung, J. D. (2017). Radiative flow of Powell-Eyring magneto-nanofluid over a stretching cylinder with chemical reaction and double stratification near a stagnation point. PloS one, 12(1), e0170790.

[18] Chhabra, R. P., & Uhlherr, P. H. T. (1980). Creeping motion of spheres through shear-thinning elastic fluids described by the Carreau viscosity equation. Rheologica Acta, 19(2), 187-195.

[19] Bush, M. B., & Phan-Thien, N. (1984). Drag force on a sphere in creeping motion throug a Carreau model fluid. Journal of non-newtonian fluid mechanics, 16(3), 303-313.

[20] Hsu, J. P., & Yeh, S. J. (2008). Drag on two coaxial rigid spheres moving along the axis of a cylinder filled with Carreau fluid. Powder Technology, 182(1), 56-71.

[21] Waqas, M., Jabeen, S., Hayat, T., Khan, M. I., & Alsaedi, A. (2019). Modeling and analysis for magnetic dipole impact in nonlinear thermally radiating Carreau nanofluid flow subject to heat generation. Journal of Magnetism and Magnetic Materials, 485, 197-204.

[22] Yousif, M. A., Ismael, H. F., Abbas, T., & Ellahi, R. (2019). Numerical study of momentum and heat transfer of MHD Carreau nanofluid over an exponentially stretched plate with internal heat source/sink and radiation. Heat Transfer Research, 50(7).

[23] Lu, D., Ramzan, M., ul Huda, N., Chung, J. D., & Farooq, U. (2018). Nonlinear radiation effect on MHD Carreau nanofluid flow over a radially stretching surface with zero mass flux at the surface. Scientific reports, 8(1), 1-17.

[24] Lu, D., Mohammad, M., Ramzan, M., Bilal, M., Howari, F., & Suleman, M. (2019). MHD boundary layer flow of Carreau fluid over a convectively heated bidirectional sheet with non-Fourier heat flux and variable thermal conductivity. Symmetry, 11(5), 618.

[25] Khan, M., Shahid, A., El Shafey, M., Salahuddin, T., & Khan, F. (2020). Predicting entropy generation in flow of non-Newtonian flow due to a stretching sheet with chemically reactive species. Computer Methods and Programs in Biomedicine, 187, 105246.

[26] Ramzan, M., Farooq, M., Alsaedi, A., & Hayat, T. (2013). MHD three-dimensional flow of couple stress fluid with Newtonian heating. The European Physical Journal Plus, 128(5), 49.

[27] Suleman, M., Ramzan, M., Zulfiqar, M., Bilal, M., Shafee, A., Chung, J. D., ... & Farooq, U. (2018). Entropy analysis of 3D non-Newtonian MHD nanofluid flow with nonlinear thermal radiation past over exponential stretched surface. Entropy, 20(12), 930.

[28] Khan, I., Malik, M. Y., Hussain, A., & Khan, M. (2017). Magnetohydrodynamics Carreau nanofluid flow over an inclined convective heated stretching cylinder with Joule heating. Results in Physics, 7, 4001-4012.

[29] Yang, L., Du, K., & Zhang, Z. (2020). Heat transfer and flow optimization of a novel sinusoidal minitube filled with non-Newtonian SiC/EG-water nanofluids. International Journal of Mechanical Sciences, 168, 105310.

[30] Lu, D. C., Ramzan, M., Bilal, M., Chung, J. D., & Farooq, U. (2018). Upshot of chemical species and nonlinear thermal radiation on Oldroyd-B nanofluid flow past a bi-directional stretched surface with heat generation/absorption in a porous media. Communications in Theoretical Physics, 70(1), 071.

[31] Hayat, T., Aziz, A., Muhammad, T., & Alsaedi, A. (2018). An optimal analysis for Darcy-Forchheimer 3D flow of Carreau nanofluid with convectively heated surface. Results in Physics, 9, 598-608.

[32] Khan, M., & Azam, M. (2017). Unsteady heat and mass transfer mechanisms in MHD Carreau nanofluid flow. Journal of Molecular Liquids, 225, 554-562.

[33] Eid, M. R., Mahny, K. L., Muhammad, T., & Sheikholeslami, M. (2018). Numerical treatment for Carreau nanofluid flow over a porous nonlinear stretching surface. Results in physics, 8, 1185-1193.

[34] Khan, M. (2016). A revised model to analyze the heat and mass transfer mechanisms in the flow of Carreau nanofluids. International Journal of Heat and Mass Transfer, 103, 291-297.

[35] Hsiao, K. L. (2017). To promote radiation electrical MHD activation energy thermal extrusion manufacturing system efficiency by using Carreau-Nanofluid with parameters control method. Energy, 130, 486-499.

[36] Darcy, H. (1856). Les fontaines publiques de la ville de Dijon: exposition et application... Victor Dalmont.

[37] Forchheimer, P. (1901). Wasserbewegung durch boden. Z. Ver. Deutsch, Ing., 45, 1782-1788.

[38] Muskat, M. (1946). The flow of homogeneous ‡uids through porous media (No. 532.5 M88).

[39] Pal, D., & Mondal, H. (2012). Hydromagnetic convective diffusion of species in Darcy–Forchheimer porous medium with non-uniform heat source/sink and variable viscosity.International Communications in Heat and Mass Transfer, 39(7), 913-917.

[40] Ganesh, N. V., Hakeem, A. A., & Ganga, B. (2016). Darcy–Forchheimer flow of hydromagnetic nanofluid over a stretching/shrinking sheet in a thermally stratified porous medium with second order slip, viscous and Ohmic dissipations effects. Ain Shams Engineering Journal, 9(4) 939-951.

[41] Alshomrani, A. S., & Ullah, M. Z. (2019). E¤ects of Homogeneous–Heterogeneous Reactions and Convective Condition in Darcy–Forchheimer Flow of Carbon Nanotubes. Journal of Heat Transfer, 141(1), 012405.

[42] Saif, R. S., Hayat, T., Ellahi, R., Muhammad, T., & Alsaedi, A. (2018). Darcy–Forchheimer flow of nanofluid due to a curved stretching surface. International Journal of Numerical Methods for Heat & Fluid Flow. DOI: 10.1108/HFF-08-2017-0301.

[43] Seth, G. S., Kumar, R., & Bhattacharyya, A. (2018). Entropy generation of dissipative flow of carbon nanotubes in rotating frame with Darcy-Forchheimer porous medium: A numerical study. Journal of Molecular Liquids, 268, 637-646.

[44] Hayat, T., Ra. . . que, K., Muhammad, T., Alsaedi, A., & Ayub, M. (2018). Carbon nanotubes significance in Darcy-Forchheimer flow. Results in Physics, 8, 26-33.

[45] Zeeshan, A., Maskeen, M. M., & Mehmood, O. U. (2018). Hydromagnetic nanofuid flow past a stretching cylinder embedded in non-Darcian Forchheimer porous media. Neural Computing and Applications, 30(11), 3479-3489.

[46] Tarakaramu, N., Narayana, P. S., & Venkateswarlu, B. (2019). MHD Three Dimensional Darcy-Forchheimer Flow of a Nanofluid with Nonlinear Thermal Radiation. In Applied Mathematics and Scientific Computing (pp. 87-97). Birkhäuser, Cham.

[47] RamReddy, C., Naveen, P., & Srinivasacharya, D. (2018). nonlinear convective flow of non-Newtonian fuid over an inclined plate with convective surface condition: a Darcy–Forchheimer model. International Journal of Applied and Computational Mathematics, 4(1), 51.

[48] Farooq, M., Ahmad, S., Javed, M., & Anjum, A. (2019). Melting heat transfer in squeezed nanofluid flow through Darcy Forchheimer medium. Journal of Heat Transfer, 141(1), 012402.

hafeez

ORIGINALITY REPORT

16%	8%	14%	4%
SIMILARITY INDEX	INTERNET SOURCES	PUBLICATIONS	STUDENT PAPERS

PRIMARY SOURCES

1	Masood Khan, Humara Sardar, M. Mudassar Gulzar, Ali Saleh Alshomrani. "On multiple solutions of non-Newtonian Carreau fluid flow over an inclined shrinking sheet", Results in Physics, 2018 Publication	2%
2	www.tandfonline.com Internet Source	2%
3	Submitted to VIT University Student Paper	1%
4	Hashim, Masood Khan, Ali Saleh Alshomrani. "Characteristics of melting heat transfer during flow of Carreau fluid induced by a stretching cylinder", The European Physical Journal E, 2017 Publication	1%
5	jafmonline.net Internet Source	<1%
6	www.nature.com Internet Source	<1%